

Enclosure 5a  
MELCOR Accident Analysis

## CONTENTS

Contents	ii
1. Introduction	1
2. General Description of MELCOR	3
2.1 Radionuclide Package in MELCOR	5
2.1.1 Suppression Pool	6
2.1.2 Spray Systems	7
2.1.3 Filters	8
3. Consideration of Phenomenological Uncertainties in MELCOR	9
4. MELCOR BWR Input Models	11
4.1 Reactor Pressure Vessel and Reactor Coolant System Models	11
4.2 Core Model	15
4.3 Residual Heat Removal System Models	18
4.4 Emergency Core Cooling Systems Models	18
4.5 Containment Model	19
4.6 Reactor Cavity Model	23
4.7 Balance of Plant Models	25
5. MELCOR Calculations for Containment Filtered Venting System Analysis	29
5.1 Case 2 (No Venting or Spray)	36
5.2 Case 3 (Wetwell Venting)	38
5.3 Case 6 (Core Sprays)	38
5.4 Case 7 (Core Sprays and Wetwell Venting)	39
5.5 Case 12 (Drywell Venting)	39
5.6 Case 13 (Drywell Venting and Drywell Sprays)	40
5.7 Case 14 (Drywell Sprays)	40
5.8 Case 15 (Drywell Sprays and Wetwell Venting)	40
5.9 Additional MELCOR Cases for Sensitivity Analysis	50
5.10 RCIC Operation Sensitivity	51
5.11 Effect of Spray	53
5.12 Combined Effect of Venting and Spray	53
5.13 Drywell Spray Sensitivity	55
6. Conclusions from MELCOR Analysis	59
7. References	61

## 1. INTRODUCTION

This enclosure documents MELCOR analysis of selected accident scenarios in a boiling-water reactor (BWR) plant with a Mark I containment in support of the staff's ongoing effort to address the Near-Term Task Force (NTTF) recommendation related to the containment venting [1]. Specifically, the work reported herein relates to the calculations of fission product release estimates using the U.S. Nuclear Regulatory Commission (NRC) severe accident analysis code MELCOR [2]. The release estimates are used to calculate health consequence and offsite property damage assessment using the MELCOR Accident Consequence Code System, Version 2, or MACCS2 [3], discussed in Enclosure 5b. The MELCOR/MACCS2 results, along with consideration of probabilistic risk assessment (PRA) as discussed in Enclosure 5c, are used in regulatory analyses of various accident prevention and mitigation strategies.

MELCOR has a long history of systematic development whereby each release version provides an update of code capabilities with regard to phenomenological modeling, code assessment, and other code improvements. The code has an extensive assessment database and is routinely benchmarked against other codes as well as experimental data. The code is also routinely subjected to rigorous quality assurance processes.

The selection of accident scenarios considered for MELCOR and MACCS analyses is informed by the recent state-of-the-art reactor consequence analysis or SOARCA [4] and also by the recent Fukushima study [5]. Specifically, two accident scenarios were selected for MELCOR/MACCS analyses as in the SOARCA Peach Bottom plant consequence analysis. These are: long-term station blackout (LTSBO) and short-term station blackout (STSBO) as defined in the SOARCA study, both initiated by a seismic event. The LTSBO results in a loss of offsite power (LOOP), failure of onsite power, and failure of the grid. All systems dependent on AC power are unavailable. The turbine-driven reactor core injection cooling (RCIC) system is available until battery depletion and, for the current study, it is assumed that the high-pressure coolant injection (HPCI) system is not available. For STSBO, it is further assumed that the RCIC is initially not available.

The primary focus is on the LTSBO scenario and a large number of MELCOR cases were run simulating different possible outcomes (e.g., containment failure by overpressurization, drywell liner melt-through, main steam line rupture). Consideration was given to various preventative and mitigative measures and how these influence the failure modes. Accident scenarios other than station blackout (SBO) were left out following the same considerations (i.e., core damage frequency cutoff, generic containment performance improvements to reduce the accident frequency or the severity of consequences, etc.) as in the SOARCA study. It is noted that the Electric Power Research Institute (EPRI), on behalf of the industry, has performed similar analysis in support of strategies for mitigating radiological releases from severe accidents at BWR Mark I and Mark II containments.

The MELCOR code calculations, described in considerable detail in the rest of this document, are deterministic in nature. The calculations produce point estimates of the quantities of interest (e.g., radionuclide release fractions). There are phenomenological uncertainties in the code and, as a result, the predicted point estimates also have some uncertainties. For the containment venting issue, the most pertinent uncertainties are related to core melt progression in a BWR in the presence of one or more mitigation measures, ex-vessel core debris behavior (e.g., molten core-concrete interaction, melt spreading), and fission product decontamination.

There are also modeling uncertainties in MACCS; in particular, those related to atmospheric transport of fission product aerosols. Given these uncertainties, the MELCOR deterministic safety analysis and MACCS consequence analysis are often supplemented by uncertainty analyses and sensitivity studies to provide a bounding estimate of the parameters of interest for regulatory analysis and decisionmaking.

Another source of uncertainty not discussed in the present report relates to that associated with the implementation of prevention or mitigation features used in the MELCOR analysis. It is assumed that in an SBO situation, such features or measures will be available. The report makes no statement, implied or otherwise, regarding the effectiveness and human reliability of operator actions in a severe accident situation; nor does it make any statement regarding equipment availability, operability, and system monitoring in a severe accident situation. These elements play a significant role in determining the feasibility and efficacy of any prevention and mitigation measures.

The report provides a discussion of the deterministic analysis of accident progression and its consequence given a core melt accident, and makes no assumption of the core damage frequency or the probability of a particular mode of failure (e.g., liner melt-through). The latter information is important for an estimation of risk and for regulatory analysis. It is provided in a separate enclosure.

Section 2 of this report provides a general description of the MELCOR code and focuses on the features of the code that are relevant for the containment venting analysis. Section 3 provides some general discussion of uncertainties in relation to MELCOR analysis of accident scenarios. Section 4 discusses the BWR MELCOR model used in the current study. As will be elaborated in this section later, the Peach Bottom SOARCA BWR model is used with a few modifications. Section 5 delineates the MELCOR calculation matrix comprising a large number of cases covering variations of LTSBO as well as various prevention and mitigation measures. This section also discusses the results of baseline MELCOR calculations and selected sensitivity cases highlighting the relative effects of various prevention and mitigation measures. Conclusions from MELCOR analysis are drawn in Section 6 of this report. Corresponding MACCS calculations and a discussion of results are provided in a separate enclosure.

## 2. GENERAL DESCRIPTION OF MELCOR

MELCOR is an integrated system-level computer code for modeling progression of severe accidents (i.e., accidents resulting in severe core damage, possibly melting of the core, leading to release of radioactivity) in nuclear power reactors. The scope of accident progression modeling includes:

- core uncover (due to loss of coolant), fuel heatup, candling, clad ballooning, clad oxidation, fuel degradation (loss of geometry), and core material melting and relocation
- heatup of reactor vessel lower head from relocated core materials, subsequent failure of the lower head from thermal and mechanical loading, and release of molten core debris to the reactor cavity
- molten core-concrete interaction in the reactor cavity and ensuing aerosol generation
- in-vessel and ex-vessel hydrogen production, transport, and combustion
- fission product (aerosol and vapor) release from the core, and transport and deposition in the containment
- containment loading from high-pressure melt ejection, overpressurization from noncondensable gas generation including hydrogen, or other mechanisms (e.g., hydrogen burning, thermal attack of liner), and subsequent failure of the containment
- fission product release into the environment

MELCOR development was started in the 1980s by the NRC to provide an estimate of risk associated with a core melt accident in nuclear power plants. The initial thrust of code development was to have an analytical tool for adequate quantification of severe accident risks, yet a reasonably fast-running code that embodied, in a parametric manner, the then state of phenomenological knowledge on severe accidents.

In the years following the initial development of MELCOR, significant advances were made to the phenomenological understanding of severe accidents as a result of extensive research both in the experimental and in the analytical fronts. This together with the advent of faster and more powerful computing capabilities facilitated further development of MELCOR in primarily two areas—development of more mechanistic modeling of severe accident phenomena and numerical improvement for a faster running code. As a result of modeling improvements, MELCOR has become the repository of an improved understanding of severe accident phenomena, and a code of choice for confirmatory safety analysis of nuclear power plants. The code has a substantial worldwide community of users, and its use has been expanded to include both power and nonpower reactors, other nuclear systems (e.g., spent fuel pool, dry cask storage), and advanced reactor concepts, including non-light-water reactor designs. The code is routinely used as a confirmatory analysis tool to provide technical basis in support of a variety of regulatory applications, including power uprate, design-basis containment performance, risk-informing loss-of-coolant accident criteria, and review of new and advanced reactor designs.

Many MELCOR models are mechanistic; however, some are parametric, particularly those related to phenomena with large uncertainties where consensus is lacking concerning an acceptable mechanistic approach. Current use of MELCOR for deterministic safety analysis is often supplemented by uncertainty analyses and sensitivity studies. To facilitate this, many of the mechanistic models have been coded with optional adjustable parameters. These parameters can be varied one at a time as well as multivariate effects can be examined in a systematic manner. This does not affect the mechanistic nature of the modeling, but it does allow the analyst to easily address questions of how particular modeling parameters affect the course of a calculated transient.

MELCOR has a modular architecture consisting of a number of “packages” that address different aspects of reactor accident analyses. The packages come in three categories: (1) basic physical phenomena (i.e., hydrodynamics, heat and mass transfer to structures, core degradation and relocation, core-structure and fuel-coolant interactions, gas combustion, and aerosol and vapor physics), (2) reactor design specific information (i.e., decay heat generation, sprays, and engineering safety systems, etc.), and (3) support functions (thermodynamics, equations of state, material properties, data-handling utilities, and equation solvers). The important phenomenological packages (first category) are listed in Table 1.

**Table 1. Important Phenomenological Packages in MELCOR**

<b>Acronym</b>	<b>Package Name</b>	<b>Functional Description</b>
BUR	Burn package	Models the combustion of gases in control volumes. The models consider the effects of burning on a global basis and are based on the deflagration models in the HECTR 1.5 code.
CAV	Cavity package	Models core-concrete interaction (an ex-vessel phenomenon) and melt spreading. The effects of heat transfer, concrete ablation, cavity shape change, and gas generation are included, using models taken from the CORCON-Mod3 code.
COR	Core package	Models thermal response of the core and lower plenum internal structures, including the portion of the lower head directly below the core. The package also models the relocation of core and lower plenum structural materials during melting, slumping, formation of molten pool and debris, failure of the reactor vessel, and ejection of debris into the reactor cavity.
CVH/FL	Control volume hydrodynamic and flow path	Models of the thermal-hydraulic behavior of water, vapor and gases in control volumes connected by flow paths, including evaporation and condensation phenomena.
FDI	Fuel dispersal package	Models both low-pressure molten fuel ejection and high-pressure molten fuel ejection from the reactor vessel, and the behavior of dispersed debris in containment (direct containment heating phenomenon).
HS	Heat structure package	Models heat conduction within an intact, solid structure and energy transfer across its boundary surfaces. The modeling capabilities of heat structures are general and can include pressure vessel internals and walls, containment structures and walls, fuel rods, steam generator tubes, piping walls, etc.

RN	Radionuclide package	Models the behavior of fission product aerosols and vapors released from fuel and debris, aerosol dynamics with vapor condensation and reevaporization, deposition on structure surfaces, transport through flow paths, and removal by engineered safety features.
----	----------------------	--

## 2.1 Radionuclide Package in MELCOR

The radionuclide (RN) package is of particular importance since the output of this package is used for dose calculations by MACCS. Within the RN package, the MELCOR code categorizes radionuclides and other pertinent materials into elemental classes that exhibit similar chemistry.

These elemental classes and their representative elements are shown in Table 2. The modeling and treatment of radionuclides in the RN package include:

- release of radionuclides from intact fuel and from core debris
- transport and deposition of radionuclide vapors and aerosols through the reactor coolant system
- behavior of radionuclides and radioactive aerosols in the reactor containment
- effects of engineered safety systems on the amount of radioactive material that can be released from the reactor containment

**Table 2. Elemental Classes and Representative Radionuclides in the RN Package**

Class #	Class Name	Representative	Member Elements
1	Noble Gases	Xe	He, Ne, Ar, Kr, Xe, Rn, H, N
2	Alkali Metals	Cs	Li, Na, K, Rb, Cs, Fr, Cu
3	Alkaline Earths	Ba	Be, Mg, Ca, Sr, Ba, Ra, Es, Fm
4	Halogens	I	F, Cl, Br, I, At
5	Chalcogens	Te	O, S, Se, Te, Po
6	Platinoids	Ru	Ru, Rh, Pd, Re, Os, Ir, Pt, Au, Ni
7	Early Transition Elements	Mo	V, Cr, Fe, Co, Mn, Nb, Mo, Tc, Ta, W
8	Tetravalent	Ce	Ti, Zr, Hf, Ce, Th, Pa, Np, Pu, C
9	Trivalent	La	Al, Sc, Y, La, Ac, Pr, Nd, Pm, Sm, Eu, Gd, Tb, Dy, Ho, Er, Tm, Yb, Lu, Am, Cm, Bk, Cf
10	Uranium	U	U
11	More Volatile Main Group	Cd	Cd, Hg, Zn, As, Sb, Pb, Tl, Bi
12	Less Volatile Main Group	Sn	Ga, Ge, In, Sn, Ag
13	Boron	B	B, Si, P
14	Water	H <sub>2</sub> O	H <sub>2</sub> O
15	Concrete	--	--
16	Cesium Iodide	CsI	CsI

17	Cesium Molybdate	Cs <sub>2</sub> MoO <sub>4</sub>	Cs <sub>2</sub> MoO <sub>4</sub>
18	Non-Radioactive Tin	Sn	Sn

MELCOR considers radionuclide release from fuel both within the reactor vessel and when reactor fuel has been expelled from the reactor coolant system into the containment. Radionuclide release from fuel within the reactor vessel can be calculated using one of three closely related models: CORSOR, CORSOR-M, and CORSOR-Booth [6]. All three of these models have an empirical relationship derived from data on tests of fission product release from fuel heated usually out of pile. Diffusion coefficients in these models have been adjusted to match more recent tests such as those being done as part of the PHÉBUS-FP project [7].

Ex-vessel release of radionuclides is done with the VANESA model [8] developed based on experimental data explicitly for this purpose. The model considers fission product release by vaporization into bubbles of gas sparging through core debris attacking structural concrete. It also considers the formation of aerosols due to the bursting of bubbles at the surface of molten core debris. Radionuclide release can be retarded substantially by the presence of a water pool over the surface of the core debris. Modeling of this attenuation of the ex-vessel release is akin to that used in MELCOR to model decontamination of aerosol-laden gas flows through steam suppression pools. The suppression pool decontamination, including uncertainties, is discussed below in more detail.

Modeling of agglomeration and deposition of aerosol particles is done in MELCOR using the MAEROS model [9]. Deposition mechanisms considered in MAEROS are: gravitational settling, diffusion, thermophoresis, diffusiophoresis, and inertial impaction. The code also models vapor deposition by condensation as well as vapor chemisorption onto surfaces. Further, a model for hygroscopicity effects is also available in MELCOR. As with any phenomenological modeling, the models in MAEROS were validated with the then available but limited data. There are underlying uncertainties in these models that need to be assessed systematically with more recent data to determine their impact on the overall release estimates. This is, however, beyond the scope of the present study.

The MELCOR code considers the decontamination effects of the containment design and engineered safety features on fission products scrubbing. Specific features that are modeled include decontamination by: (1) suppression pool, (2) spray systems, and (3) filters. Details of the modeling are discussed in the following paragraphs.

### 2.1.1 Suppression Pool

Pool scrubbing is a relevant issue in nuclear safety since it provides a means to reduce source term to the environment during hypothetical severe accidents. Several severe accident scenarios involve the transport paths of fission product aerosols which include passages through stagnant pools of water where pool scrubbing can occur. Although the pressure suppression pool in BWRs is primarily designed to avoid overpressurization of the wetwell space, scrubbing in such pools has been given credit for mitigating the source term and hence the associated risk posed by accidents.

Several fundamental processes take place during aerosol pool scrubbing: diffusiophoresis, thermophoresis, inertial impaction, gravitational settling, centrifugal deposition, diffusion during bubbles rise, Brownian diffusion, etc. Aerosol characteristics (i.e., size, hygroscopicity, etc.) are

the key factors for the effectiveness of these removal processes. Gas hydrodynamics plays an essential role determining key variables for pool scrubbing such as bubbles size and surface/volume ratio. In addition, other parameters like pool depth (injection point submergence), water subcooling, carrier gas composition and temperature and velocity, injection mode, water composition, etc., heavily influence individual pool scrubbing processes. In addition to the main aerosol removal processes, change in the particle size directly affects the pool scrubbing.

Decontamination by a steam suppression pool is done with the SPARC-90 model [10]. This model calculates removal of both aerosol and iodine gas from gases sparging through the suppression pool. Pool scrubbing or wet scrubbing is the removal of aerosol particles in gas bubbles rising in a water pool. The pool thus acts as a filter. Traditionally, the scrubbing efficiency has been expressed in terms of a decontamination factor (DF), which is defined by the ratio of the aerosol mass flow rate entering ( $m_{in}$ ) and leaving ( $m_{out}$ ) the pool. The path of aerosols along the pool height is usually split into three regions: injection (bubble formation) region, bubble rise region, and pool surface (bubble collapse) region. The overall DF is a multiplication of individual DFs of the three regions of the pool.

Past investigations have shown that decontamination by bubble formation and equilibration in a water pool can be significant, both in BWR's and PWR's risk relevant sequences. For shallow pools, the relative significance of the bubble formation and equilibration processes in determining the decontamination can be even larger than that by the decontamination process during the bubble rise through the pool height. Past investigations have also shown that the DF displays an inverted Gaussian type of trend as a function of particle diameter with a minimum at about 0.1  $\mu\text{m}$ . Uncertainties in the particle size distribution at the inlet can largely influence DF estimates. Also, the DF increases smoothly and exponentially with submergence. Increased gas residence time through the pool efficiently raises the DF. WASH-1400, "The Reactor Safety Study," assumed a DF of 100 for subcooled pools and 1 for saturated pools.

### **2.1.2 Spray Systems**

The drywells of most BWRs are equipped with water spray systems. These spray systems were installed to condense steam and reduce the pressure of the containment or drywell atmosphere in the event of a design-basis break in the reactor coolant system. Sprays are also very effective at removing aerosol particles from the containment or drywell atmospheres during severe reactor accidents. The spray systems consist of a large number of spray nozzles oriented differently near the top of the containment or drywell, and the header and spray nozzle configurations were designed for optimum spray pattern and droplet size with flows of several thousand gallons per minute to the drywell and several hundred gallons per minute to the suppression chamber. These nozzles discharge large numbers of water droplets that fall along ballistic trajectories through the atmosphere and sweep out aerosol particles.

Spray droplets remove aerosol particles from the containment or drywell atmospheres by several mechanisms:

- diffusiophoresis: steam condensing on the droplets and sweeping aerosol particles
- impaction: aerosol particles colliding with the droplet
- interception: aerosol particles adhering to the droplets
- diffusion: Brownian motion carrying aerosol particles in contact with falling droplets

The diffusiophoresis mechanism is only important early in an accident when the atmosphere is steam rich and aerosol concentrations are quite low. Consequently, this mechanism is not usually considered in the analysis of the steady state effectiveness of aerosol removal by sprays. The efficiency of aerosol removal by impaction, interception, and diffusion is expressed as the ratio of the number of particles actually removed from the atmosphere by a particular mechanism to the number of fixed particles that would be removed by a droplet along the same trajectory.

The removal efficiency is highly dependent on both the particle size and the effective droplet diameter. Diffusion is effective at the removal of very small aerosol particles ( $<0.1 \mu\text{m}$ ). Impaction affects mostly aerosol particles larger than about  $5 \mu\text{m}$ . Interception affects particles in the size range of  $0.5$  to  $2 \mu\text{m}$ . Consequently, there is a minimum in the total aerosol removal efficiency when plotted against aerosol particle size. This minimum depends on the droplet diameter.

Reductions in the aerosol concentration by a factor of 10 can initially be achieved within 1 hour with full design spray flow. Further reduction in the aerosol concentration can be slower because the action of the spray alters the size distribution of the aerosol so that particles are less efficiently removed.

### **2.1.3 Filters**

The requirements for the design of a filter system in removing the fission products depend on the thermal-hydraulic conditions (temperature, pressure, humidity, flow rate through the filter system) and concentration of the fission products in gaseous and aerosol form. Containment or auxiliary (reactor) building filtration systems are designed to avoid any substantial release of activity transported by aerosol particles and gaseous iodine. Of course, the main assumption here is that the containment is isolated and there are no uncontrolled leak paths.

As a result of the emerging new regulatory requirements for severe accidents, new filtration concepts were developed starting in the 1980s to backfit the current operating reactors in some countries. The main emphasis in the new regulatory requirements is to minimize potential land contamination by keeping the pressure in the containment under the design limits in order to avoid catastrophic containment failures and gross penetration leakage. This is done by venting through a containment filtered vent which should, at the same time, remove the aerosol particles and molecular gaseous iodine with certain efficiencies.

For most filtration devices, the efficiency of collection depends strongly on the particle size. For the purpose of MELCOR/MACCS analysis, the efficiency of filters is characterized by a specified DF. Further discussion of filter efficiency is provided in Section 5 of this report. For wetwell venting where the fission product aerosols are already scrubbed by the suppression pool, thus altering their size distribution, the DF range for filter is assumed to be relatively low. In the MACCS analysis reported in Enclosure 5b, the assumed range of DF is between 2 and 10. Some calculations were performed with a DF of 100. For drywell venting, if the feature is present in the design, a much higher DF (on the order of 1,000) may be attributed to the filter since the aerosols are not pre-scrubbed.

### 3. CONSIDERATION OF PHENOMENOLOGICAL UNCERTAINTIES IN MELCOR

MELCOR is considered a state-of-the-art code for severe accident modeling and analysis, and it has reached a reasonably high level of maturity over the years as evidenced from its wide acceptability and its broad range of applications. Nevertheless, it is important to recognize the phenomenological uncertainties in MELCOR and their significance to MELCOR results. Moreover, it is important to understand the compounding effect of various uncertainties on the ultimate parameter of interest i.e., source term for all practical purposes. Some of the more important uncertainties are briefly discussed in this section.

The in-vessel melt progression modeling in MELCOR starting with the loss of intact core geometry to clad oxidation, in-vessel hydrogen generation, molten core relocation to lower plenum, and subsequent lower head failure are based on experiments which were conducted with the primary objective of gaining an understanding of these phenomena in relation to the observation and experience from plant accidents such as Three Mile Island. There are uncertainties associated with these phenomena. For example, the clad oxidation model in MELCOR is predicated on certain minimum thickness of pre-oxidized clad layer and certain minimum clad temperature. Any change in the values of these parameters may have an impact on the quantity of in-vessel hydrogen generation, melt temperature, and lower head failure timing.

MELCOR lacks a mechanistic model for evaluating fuel mechanical response to the effects of clad oxidation, material interactions (i.e., eutectic formation), zircaloy melting, fuel swelling, and other processes that occur at very high temperatures. The code uses a simple temperature-based criterion to define the threshold beyond which normal ("intact") fuel rod geometry can no longer be maintained, and the core materials at a particular location collapse into particulate debris. The temperature-based criterion attempts to bound uncertainties in phenomenological processes that affect fuel rod integrity.

The rate of movement of radial molten and solid debris to the center of the core and the time it takes the debris to move to the lower plenum are controlled by the relocation time constant parameter in MELCOR. This parameter is used as a surrogate for the broad uncertainty in the debris relocation rate into water in the lower head. This, in turn, affects the potential for debris coolability in the lower head (faster relocation rates decrease coolability; slower rates improve coolability). Debris relocation in MELCOR occurs when the lower core plate in a ring yields. Molten material and particulate debris from the ring immediately moves toward the center of the core and falls into the lower head. Thus, adjustments in this relocation time constant parameter affect the overall rate at which debris enters the lower head after support plate failure. For MELCOR calculations reported in this document, the relocation time constant value in the SOARCA study was used.

As in the case of in-vessel melt progression, the ex-vessel phenomenological modeling is based on experiments which were conducted to gain an understanding of melt spreading on the drywell floor, debris quenching in the presence of water, and molten core-concrete interaction, among others. The dominant mechanism of containment failure in accident sequences such as the LTSBO, is thermal failure (melting) of the drywell liner following contact with molten core debris (i.e., drywell liner melt-through). Containment failure by this mechanism occurs after debris is released from the reactor vessel lower head and flows out of the reactor pedestal onto the main drywell floor. The precise conditions under which core debris would flow out of the

pedestal and across the drywell floor are uncertain. These uncertainties are currently captured in MELCOR in a parametric manner.

Gaseous iodine remains an uncertain source term issue in MELCOR, especially with respect to long-term radioactive release mitigation issues after the comparatively much larger airborne aerosol radioactivity has settled from the atmosphere. Mechanistic modeling of gaseous iodine behavior is a technology still under development with important international research programs to determine the dynamic behavior of iodine chemistry with respect to paints, wetted surfaces, buffered and unbuffered water pools undergoing radiolysis, and gas phase chemistry.

Partitioning the initial core inventory of cesium and iodine among certain allowable chemical forms (for release and transport) is managed within MELCOR input files that define the initial spatial mass distribution of each chemical species and its associated decay heat. Changes to the mass fractions assumed for a particular chemical group directly affect the mass fractions of other chemical groups. Due to the complexity of this general modeling uncertainty, five alternative sets of MELCOR input files are used to span the range of plausible combinations of chemical forms of key radionuclide groups.

Several other sources of phenomenological uncertainties, not specifically discussed here, may be present in MELCOR. Moreover, there are uncertainties in modeling various mitigation features described previously (e.g., drywell spray effectiveness, suppression pool scrubbing decontamination factor, and external filter efficiency). Given these various sources of uncertainties, the MELCOR prediction of the source term can have a wide range and it is not uncommon to find an order of magnitude or more variation. A comprehensive MELCOR uncertainty analysis is being done for SOARCA Peach Bottom LTSBO.

## 4. MELCOR BWR INPUT MODELS

The BWR input models described here follow the “best practice” used in the SOARCA study and reflect current understanding in severe accident modeling with the capability for modeling full-power steady-state operating conditions. The models were informed by the recent Fukushima study. The Peach Bottom SOARCA input deck was used as the baseline and a few modifications were made to the deck for the present containment venting study. These modifications are described later in appropriate subsections. The present study focuses on BWR Mark I containments. It is recognized that there are differences in design details between Mark I and Mark II containments so the results from this study may need to be appropriately qualified for Mark II containment types.

### 4.1 Reactor Pressure Vessel and Reactor Coolant System Models

Excluding the core region, the reactor pressure vessel is represented by 7 control volumes, 9 flow paths, and 24 heat structures. Nodalization for the core region between the core top guide and the bottom of active fuel are described later in the text. Figure 1 shows a representation of the MELCOR control volumes and flow paths for the reactor coolant system. Figure 2 provides a reactor vessel nodalization detail comparing MELCOR modeling features to actual vessel design. Control volumes are indicated by “CV” followed by the three-digit control volume number, and flow paths are indicated by “FL” followed by the three-digit flow path number.

The reactor pressure vessel is modeled with seven control volumes outside of the core region:

- lower plenum (CV320)
- downcomer (CV310)
- shroud dome or upper plenum (CV345)
- steam separators (CV350)
- steam dryers (CV355)
- steam dome (CV360)
- jet pumps (CV300)

The downcomer control volume (CV310) represents the volume between the core barrel and reactor vessel wall (excluding jet pump volume) from the baffle plate to the top of the steam separators. The downcomer control volume includes all volume external to the steam separators in the region above the core shroud dome. The lower plenum control volume (CV320) includes all reactor vessel volume below the bottom of active fuel excluding the downcomer region and jet pumps. All volume internal to the 20 jet pumps is represented by CV300.

Reactor vessel upper internals are modeled in detail. Four control volumes, linked in series, are used to represent changes in the quality and temperature of core exit gases as they travel from the top of the core to the main steam line nozzles. The shroud dome control volume (CV345) represents the upper mixing plenum within the core shroud dome (from the top of the core top guide to the top of the shroud dome). The steam separators control volume (CV350) comprises the steam separator standpipes and the steam separators. The steam dryer region is represented by CV355 and includes all volume inside of the dryer skirt and the dryers from the top of the steam separators to the top of the steam dryers. Water stripped from steam in the separators and dryers is returned to the downcomer volume. The reactor vessel steam dome

control volume (CV360) includes the dome region of the reactor vessel above the downcomer and steam dryer volumes.

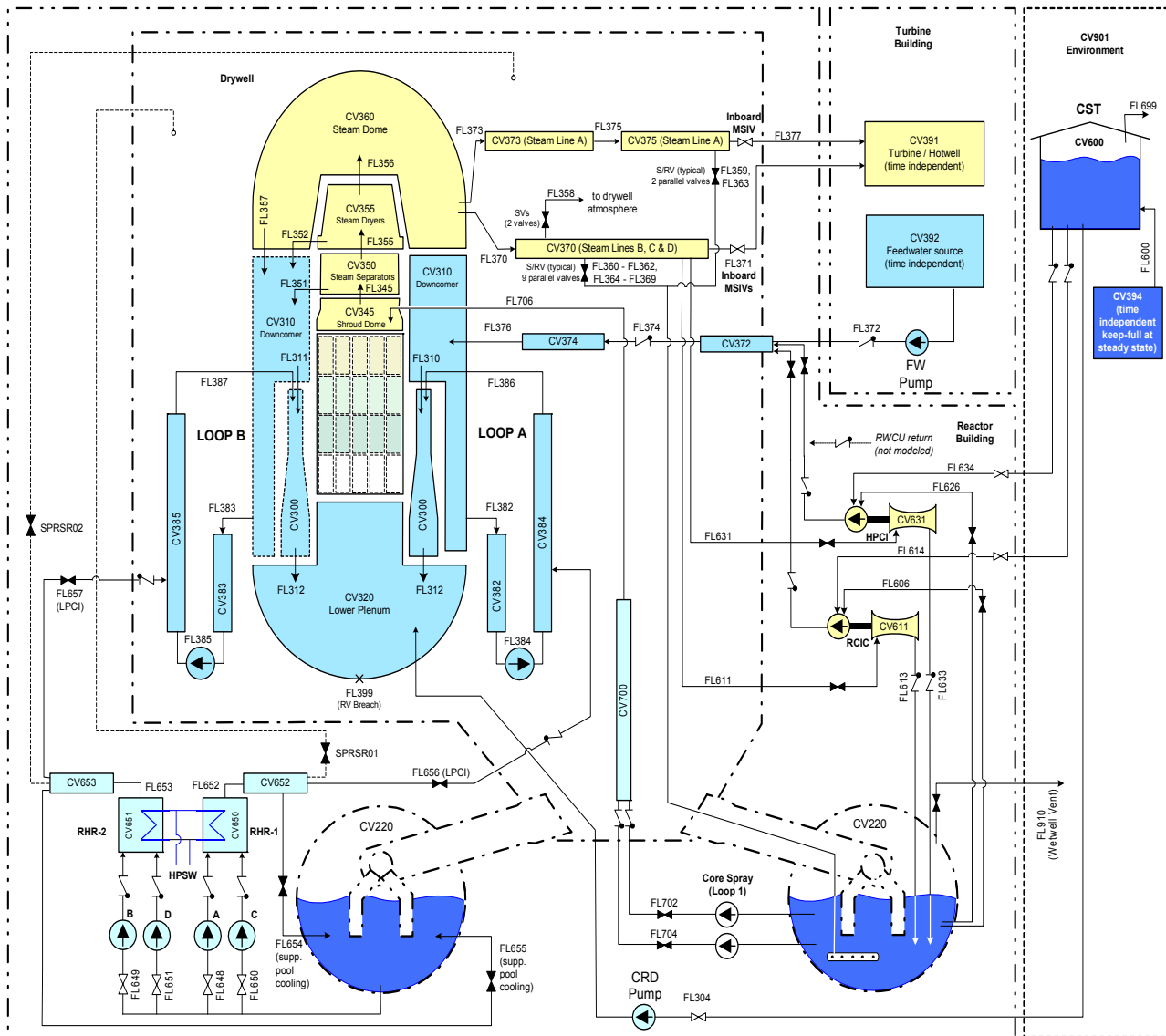


**Figure 1. MELCOR control volumes and flow paths for the reactor coolant system**

Flow paths are designed to represent all potential fluid pathways between the control volumes defined above. The nine flow paths modeled connecting reactor pressure vessel control volumes include flow between:

- the jet pumps and lower plenum (FL312)
- the shroud dome/upper plenum and steam separator standpipes (FL345)
- the steam separators and steam dryers (FL355)
- the steam dryers and steam dome (FL356)
- the steam dome and downcomer (FL357)
- Loop A suction flow from the downcomer to the jet pumps (FL310)

- Loop B suction flow from the downcomer to the jet pumps (FL311)
- the steam separators and downcomer (FL351)
- the steam dryers and downcomer (FL352)

The heat capacity and radionuclide deposition surface of a number of structures associated with the reactor pressure vessel are modeled via heat structures. The reactor pressure vessel itself is represented by four heat structures that include:

- the cylindrical portion in the lower downcomer region (HS31001)
- the cylindrical portion in the upper downcomer region (HS31011)
- the cylindrical portion adjacent to the steam dryers (HS36003)
- the hemispherical upper head (HS36002)

Cylindrical HS31001 is bounded by the downcomer (CV310) on the inside surface and the lower drywell (CV200) on the outside surface, and models the reactor vessel from the base of the downcomer to the elevation of the reactor building floor. Cylindrical HS31011 is bounded by the downcomer (CV310) on the inside surface and the mid-drywell (CV201) on the outside surface and models the reactor vessel from the elevation of the reactor building floor to the top of the steam separators. Cylindrical HS36003 is bounded by the steam dome (CV360) on the inside surface and the mid-drywell (CV201) on the outside surface and models the remaining cylindrical region of the reactor vessel from the top of the steam separators to the start of the hemispherical upper head. Hemispherical HS36002 is bounded by the steam dome (CV360) on the inside surface and the mid-drywell (CV201) on the outside surface, and models the hemispherical region of the upper head. The reactor vessel lower head is modeled within the core package and not included as a heat structure.

The core shroud is represented by 17 heat structures. Core shroud heat structures below the downcomer region represent the lower core shroud (HS32004) and the core shroud support (HS32003). Each of these structures is bounded by the lower plenum (CV320) on both surfaces. The upper shroud and dome are modeled by three heat structures. The first two structures represent the cylindrical region of the dome from the top of active fuel to the top of the core top guide (HS33017) and from the top of the core top guide to the hemispherical head (HS33018). The shroud dome head (HS34501) is represented by a horizontal rectangular heat structure. Both of these structures are bounded by the upper plenum (CV345) on the inner surface and the downcomer (CV310) on the outside surface.

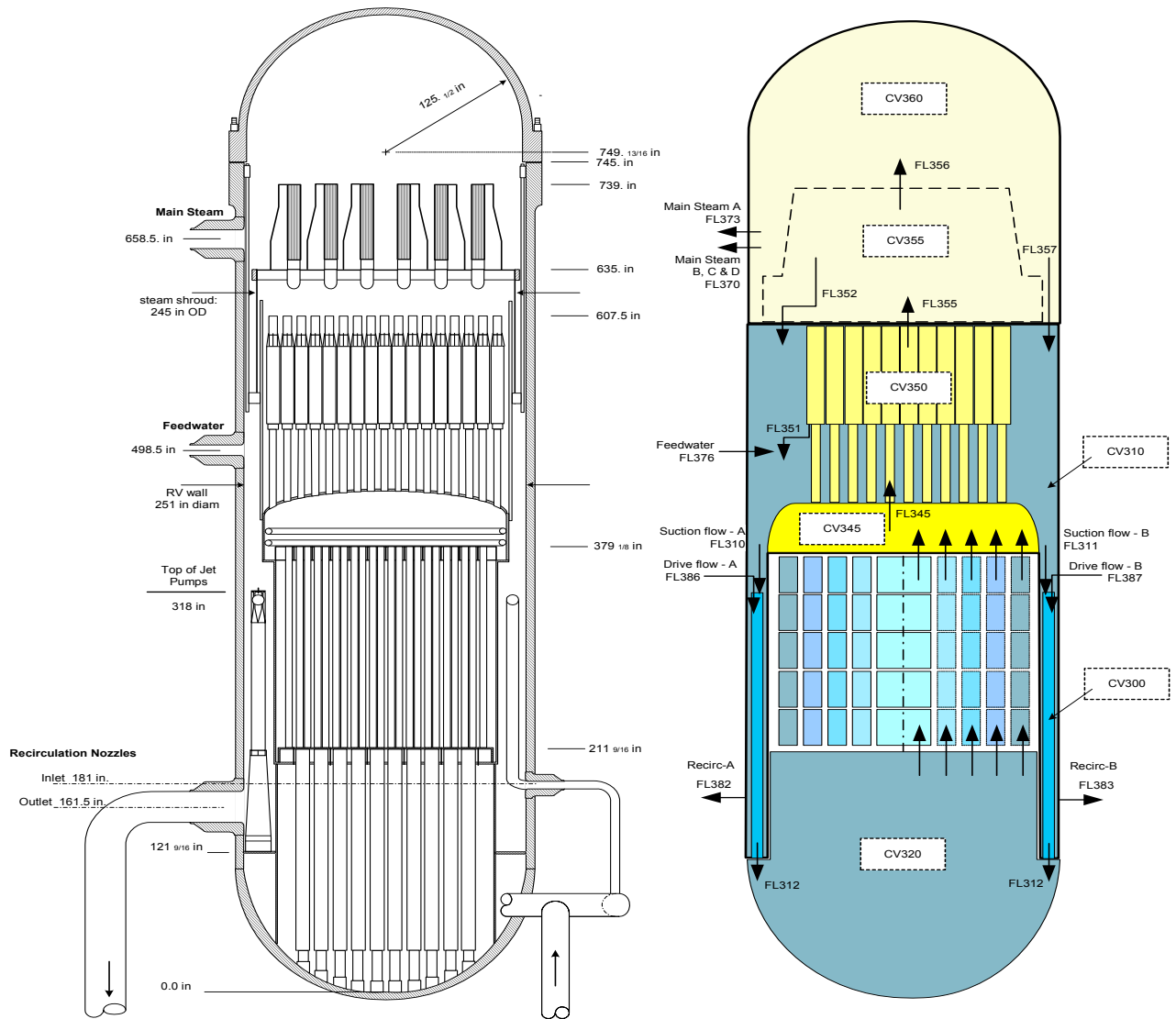


**Figure 2. Reactor vessel nodalization detail**

Three additional heat structures model other miscellaneous structures within the reactor vessel:

- the shroud baffle (HS31002)
- the standpipes and steam separators (HS35003)
- the steam dryers (HS36001)

The shroud baffle (HS31002) represents the boundary between the base of the downcomer (CV310) and the lower plenum (CV320). It is modeled by a rectangular heat structure (slab) with a surface area representing the base of the downcomer between the core shroud and reactor vessel (excluding the jet pumps). Vertical cylindrical heat structure 35003 represents the standpipes and steam separators and is bounded by the steam separators volume (CV350) on the inner surface and the downcomer (CV310) on the outer surface. Vertical rectangular

heat structure 36001 represents the steam dryers and is bounded by the steam dryer volume (CV355) on one surface and the steam dome (CV360) on the other surface.

## **4.2 Core Model**

In MELCOR, the region tracked directly by the COR package model includes a cylindrical space extending axially from the inner surface of the vessel bottom head to the core top guide and radially from the vessel centerline to the inside surface of the core shroud. The region tracked by the COR package also includes the region of the lower plenum outside of the core shroud and below the downcomer. The core and lower plenum regions are divided into concentric radial rings and axial levels. A particular radial ring and a particular axial level define a core cell (node) whose cell number is defined as a three digit integer IJJ, where the first digit represents the radial ring number and the last two digits represent the axial level number. Core cell number 314 specifies a cell located in radial ring three and axial level 14. The numbering of axial segments begins at the bottom of the vessel. Each core cell may contain one or more core components, including fuel pellets, cladding, canister walls, supporting structures (e.g., the lower core plate and control rod guide tubes), nonsupporting structures (e.g., control blades, the upper tie plate and core top guide) and particulate debris.

The MELCOR core nodalization for the current containment filtered venting study is very similar to that of the SOARCA analysis as shown in Figure 3. The entire core and lower plenum regions are divided into six radial rings and 17 axial segments. Axial levels 1 through 6 represent the entire lower plenum and the unfueled region of the core immediately above the lower core plate. Initially this region has no fuel and no internal heat source. However, during the core degradation phase, the fuel, cladding and other core components may enter the lower plenum in the form of particulate or molten debris by relocation from the upper core nodes. Axial node 6 represents the steel associated with assembly lower tie plates, fuel nose pieces and the lower core plate and its associated supports. Particulate debris formed by fuel, canister, and control blade failures above the lower core plate will be supported at this level until the lower core plate yields. Axial segments 7 through 16 represent the active fuel region. All fuel is initially in this region and generates the fission and decay power. Axial level 17 represents the nonfuel region above the core, including the top of the canisters, the upper tie plate and the core top guide. Radial ring 6 represents the region in the lower plenum outside of the core shroud inner radius and below the downcomer region.

Core cell geometry and masses for nonfuel-related core components (e.g., control rod guide tubes, lower core plate, core top guide) are obtained from a variety of references. Axial level 1 through 5 in rings 1 through 5 contains control rod stub tubes, control rod drives, and instrument guide tubes. Axial level 1 includes the region from the lower head to the top of the control rod stub tubes. Control rod stubs are modeled as tubes with a specified inner diameter and an outer diameter. Control rod drives are modeled as a solid shaft with a specified diameter representative of a BWR Mark I design. Fifty-five instrument tubes are modeled with each one including a guide tube with a specified inner diameter and an outer diameter, and a central shaft with a specified diameter. Control rod stub/drive and instrument tubes are distributed between the rings. The combined mass of the control rod stub tubes, control rod drives, and instrument tubes within axial level 1 are modeled as a stainless steel supporting structure. The surface area for this component is modeled as the outer surface area of the control rod stub tubes. Axial level 1 in ring 6 does not contain any core components.

Axial level 6 in rings 1 through 5 includes the fuel support pieces, lower core plate, lower core plate support structures and fuel assembly lower tie plates. The total mass for the fuel support pieces and lower core plate is distributed between the core rings based on the fraction of the area inside of the core shroud represented by the ring. Assembly lower tie plate mass depends on the type of fuel assemblies modeled, and is distributed based on the number of assemblies per ring. The combined mass of these structures is modeled as a steel support structure representing the lower core plate.

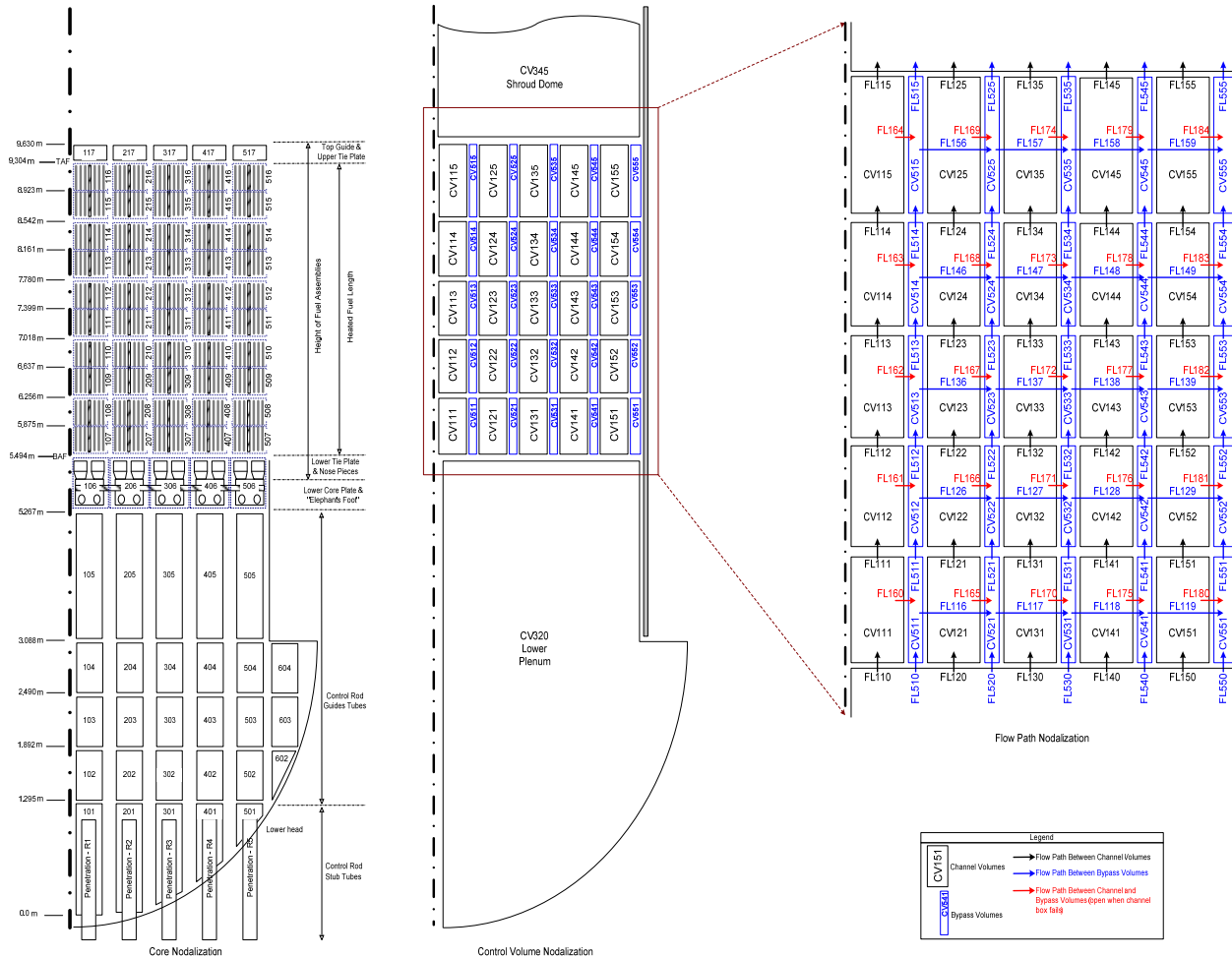


**Figure 3. MELCOR core nodalization for the containment filtered venting study**

All control blades are assumed to be inserted in the core region, regardless of the transient time (before or after SCRAM) or the type of transient (normal, ATWS). Axial levels 7 through 16 in rings 1 through 5 contain the control blades distributed as described in axial level 1. The combined stainless steel and B<sub>4</sub>C mass is modeled as a nonsupporting structure in MELCOR with the surface area estimated from control blade dimensions.

Axial level 17 in rings 1 through 5 contains the core top guide and the fuel assembly upper tie plates. The total mass for the core top guide is distributed between the core rings based on the

fraction of the area inside of the core shroud represented by the ring. Assembly upper tie plate mass depends on the type of fuel assemblies modeled, and is distributed based on the number of assemblies per ring. The combined mass of these structures is modeled as a nonsupporting steel structure.

Core cells within the five concentric rings modeling the active fuel region and the core top guide from axial levels 7 through 17 are coupled with a total of 40 hydrodynamic control volumes. Within each radial ring, five axially-stacked control volumes represent coolant flow through the core channels and five parallel (axially-stacked) control volumes represent the neighboring bypass regions of the core. This reflects a coupling between core cells and hydrodynamic control volumes within the core region.

Four distinct groups of flow paths are modeled to represent all potential flow within the core region. Axial core flow within the fuel assemblies is modeled with the channel flow area for each ring excluding flow area internal to the water rods. Axial flow paths from the lower plenum into the fuel assembly channel include pressure losses associated with flow through the fuel support piece orifices and the lower tie plate. Form losses in these core entry axial flow paths are fixed to match total core pressure drop data. Axial flow paths between volumes within the core region include friction losses for flow through fuel rods over a volume-center to volume-center length and form losses based on grid spacers. Axial flow from the upper fuel region control volume and the upper plenum includes form losses for flow through the upper tie plate. The MELCOR axial flow blockage model is activated for each of these flow paths. Axial bypass core flow between canisters and through the peripheral bypass is modeled with the bypass flow area in the core region, including flow area internal to the water rods.

At each axial level of the core, the possibility of coolant cross-flow between channel and bypass areas is modeled by horizontal flow paths. The open fraction for these flow paths are connected to control logic that monitors channel box integrity (i.e., the flow paths are closed when the channel box is intact and open if the channel box fails in a particular ring). In addition, coolant cross-flow between bypass regions is modeled by horizontal flow paths between each ring at each axial level.

The lower head is modeled as a hemisphere with an inner radius and thickness representative of a BWR Mark I plant. The lower head region extends to the downcomer baffle plate where it connects with the reactor pressure vessel. The hemispherical region of the lower head is represented by eight segments, and the cylindrical region of the lower head below the baffle plate by a single segment. A one-dimensional model of the stress and strain distribution in the lower head is applied. The temperature at which the yield stress in the lower head vanishes is set to 1,700°K to ensure creep-rupture of the lower head when it reaches the steel melting point. Heat transfer coefficients from particulate debris to the lower head and penetrations are modeled with a temperature-dependent control function which reflects conduction-based heat transfer through a frozen crust at temperatures of 2650 K and below, a conduction enhanced heat transfer coefficient as the debris reaches the eutectic melting temperature of  $\text{UO}_2$  and  $\text{ZrO}_2$ , and a convective heat transfer coefficient as the debris exceeds the eutectic melting temperature and forms a circulating molten pool.

A single lower head penetration is modeled within each of the five inner most radial rings. This penetration models the heat capacity, surface area, and axial conduction area of a single control

rod stub tube (excluding the drive shaft). By default, the penetration failure model is deactivated and the lower head failures occur due to creep rupture.

### **4.3 Residual Heat Removal System Models**

Major modes of the residual heat removal (RHR) system are included in the MELCOR model. These include low-pressure coolant injection (LPCI), drywell sprays, and suppression pool cooling. Each train of RHR is modeled separately to allow for the possibility that under certain circumstances, one train might be aligned for operation in a different mode. The model for each train includes options for operating one or two trains of pumps and heat exchangers. RHR heat exchangers operate in all modes of operation whenever high-pressure service water (HPSW) is available. RHR pumps trip under the following conditions:

- loss of ac power
- suppression pool temperatures exceed pump NPSH limits
- suppression pool level below pump suction vortex limits
- pump failure flags in the sequence trip file

RHR operation in LPCI mode draws water from the suppression pool and delivers it to the reactor vessel via the recirculation loop discharge lines upstream of discharge valves on each RHR side. The LPCI model allows for automatic or manual initiation of the system. Automatic initiation of LPCI occurs upon receipt of a reactor vessel Low-level 1 signal. LPCI is terminated when the RCIC shutdown criterion is reached (operators are assumed to shut down LPCI when this criterion is reached). Suppression pool cooling mode draws water from the suppression pool, delivers it through the RHR pumps and heat exchangers for cooling, and returns it to the suppression pool.

Drywell sprays are modeled separately from the LPCI and shutdown cooling modes of operation using the MELCOR Containment Sprays package. The suppression pool is modeled as the source control volume with the mid-drywell (CV201) modeled as the location of the spray header for RHR train I and the lower-drywell (CV200) modeled as the location of the spray header for RHR train II. Drywell spray temperatures are calculated based on suppression pool temperatures and RHR heat exchanger operation. The drywell sprays mode of RHR allows for automatic or manual initiation of the system. Manual operation of drywell sprays may be specified through single initiation and termination times. Automatic initiation of drywell sprays (assuming operator actions to follow emergency procedures) is determined based on generic spray actuation limits provided in the BWROG Emergency Procedure Guidelines:

- drywell atmosphere temperatures exceed 350°F
- drywell pressures below 3.0 psig @ 0°F, 3.0 psig @ 100°F and 7.2 psig @ 350°F

### **4.4 Emergency Core Cooling Systems Models**

Three emergency core cooling systems (ECCS) models are included in MELCOR. They include the reactor core isolation cooling (RCIC) system, the high-pressure coolant injection (HPCI) system and the low-pressure core spray (LPCS) system.

Operation of the turbine-driven RCIC system is modeled in detail. Nodalization for the RCIC system includes:

- the RCIC turbine (CV611)
- flow from main steam line C to the RCIC turbine (FL611)
- flow from the RCIC turbine to the suppression pool (FL613)
- flow from the CST to feedwater piping including the RCIC pump (FL614)
- flow from the suppression pool to feedwater piping including the RCIC pump (FL606)

The model includes a constant-flow pump, delivering 600 gpm via velocity-specified flow paths, with suction initially aligned to the CST. Switchover of pump suction to the suppression pool occurs upon receipt of a low CST water level signal. Within the MELCOR model, CRDHS suction is modeled at an elevation common to the RCIC/HPCI suction header and also accesses this dedicated volume. The RCIC system nodalization does not include heat structures.

Steam flow through the RCIC turbine is modeled to account for the transfer of energy from the steam line to the suppression pool during RCIC operation. The flow of steam from main steam line to the RCIC turbine is modeled as a function of the pressure difference between the main steam line and the suppression pool. RCIC is modeled with automatic initiation and termination criterion. RCIC is initiated on receipt of a reactor vessel low level-2 signal. RCIC is terminated on receipt of a reactor vessel high level-8 signal. User input (CF937) may also be selected to model manual pump operation where operators throttle the RCIC turbine/pump to maintain water levels after automatic initiation.

Upon receipt of a RCIC actuation signal, the RCIC pumps reach full flow after a 30 second delay and 1 second ramp up in flow. The duration of dc power (station batteries) is specified by CF901 in the sequence trip input file. When the pump is manually operated, user input may also be selected so that RCIC turbine/pump operation continues at its current speed when station batteries are depleted (CF933).

The LPCS system in the plant consists of two loops, each with two pumps, which draw suction from the suppression pool and deliver flow to the reactor vessel via a spray header just above the core. One loop (i.e., 2 pumps) of the low-pressure core spray system is modeled, with pump suction aligned to the suppression pool. Nodalization for the LPCS system includes:

- LPCS discharge piping from the LPCS pumps to spray header (CV700)
- flow from the suppression pool to LPCS piping including LPCS Pump A (FL702)
- flow from the suppression pool to LPCS piping including LPCS Pump C (FL704)
- flow from LPCS piping to the spray header in the shroud dome (FL706)

LPCS operation is modeled with two modes of operation. LPCS delivery to the reactor vessel requires a low reactor vessel pressure permissive of 400 psig. LPCS pumps start immediately upon receipt of an actuation signal. In mode one, LPCS is terminated when the RCIC shutdown criterion is reached (operators are assumed to shut down LPCS when this criterion is reached). In mode two, the operators are assumed to throttle pump speed to maintain level just above the top of the core.

#### **4.5 Containment Model**

The primary containment is subdivided into six distinct control volumes. The drywell is represented by four control volumes:

- the region internal to the reactor pedestal including the drywell sumps (CV205)
- the region external to the drywell pedestal from the floor to an elevation of 165' (CV200)
- the region from 165 feet to the drywell head flange (CV201)
- the region above the drywell head flange (CV202)

One control volume represents the vent pipes and downcomers connecting the drywell to the wetwell (CV210), and one control volume represents all remaining volume within the wetwell (CV220). The MELCOR nodalization of the primary containment is shown in Figure 4.

A total of 17 flow paths represent intact containment flow pathways. Of these, two flow paths (FL200 and FL202) connect the three drywell regions external to the reactor pedestal. Each of these flow paths is modeled with 50 percent of the interfacing flow area between the control volumes. This assumes a 50 percent obstruction by equipment and structures of the interface between the drywell regions.

Three flow paths (FL014, FL015, and FL016) connect the reactor pedestal to the lower drywell. The open fraction of the personnel doorway is reduced based on the core debris elevation in the reactor pedestal after vessel failure (debris elevation determined from CAV package). Two additional flow paths (FL012 for flow from the drywell to the vent pipes and FL017 for nominal drywell leakage from the lower drywell to the reactor building) represent flow from the drywell. Flow path 012 includes flow from the drywell into all eight vent pipes in the drywell. The nominal drywell leakage flow area, friction, and form losses are defined to match the nominal drywell leak rate. The elevation of nominal drywell leakage is modeled at the dominant location of drywell penetrations.

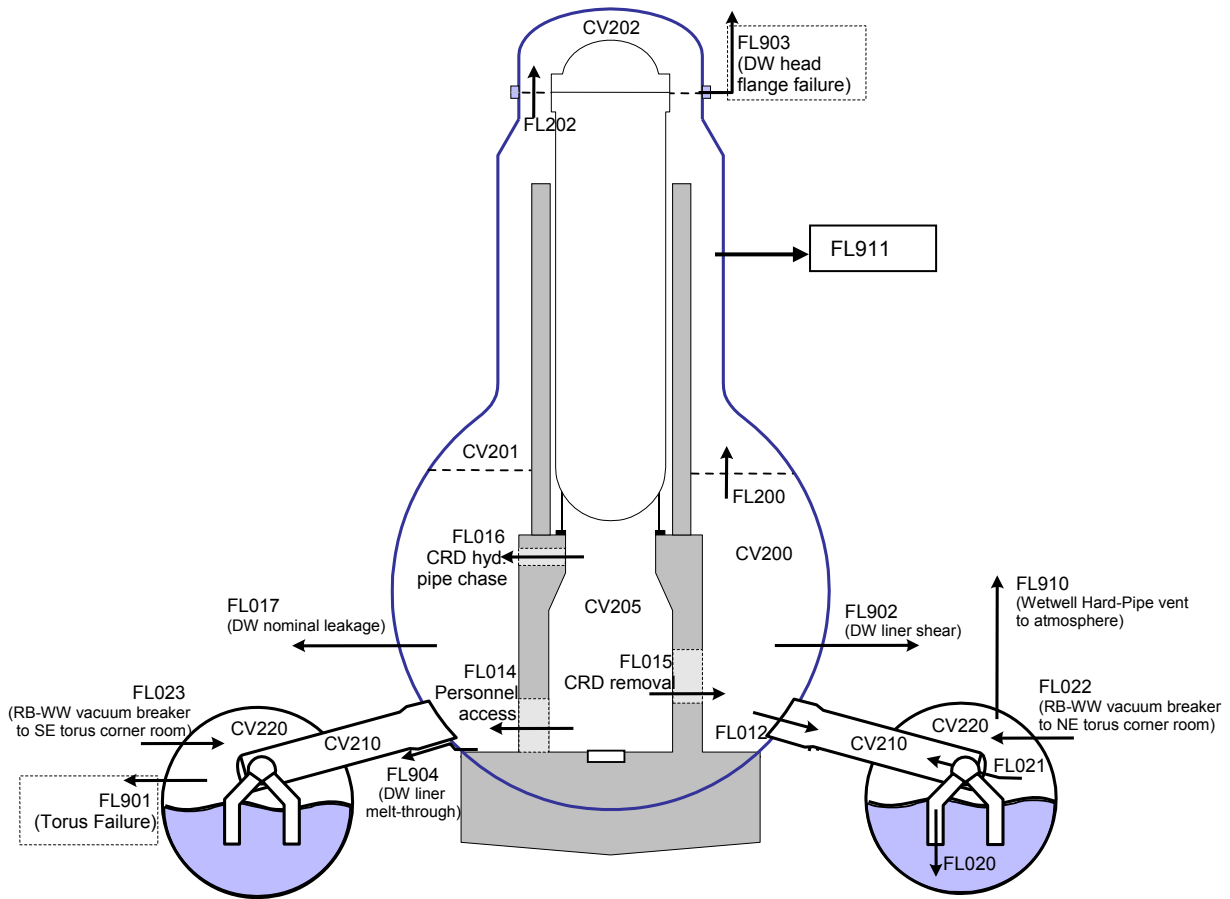


**Figure 4. MELCOR nodalization of the primary containment**

A single flow path represents flow from the downcomer pipes to the wetwell (FL020). The exit of this flow path has the SPARC pool fission product scrubbing model activated within MELCOR for aerosols and vapors across all fission product classes.

Three flow paths (FL021, FL022, and FL023) model vacuum breakers intended to limit under-pressure failures of the drywell and wetwell. The wetwell-drywell vacuum breakers open whenever the wetwell pressure exceeds the vent pipe pressure by 0.5 psid. The reactor building-wetwell vacuum breakers connect the wetwell airspace with the northeast and southeast torus corner rooms, and open whenever the pressure in the wetwell drops 2 psi below the pressure in the reactor building.

One additional flow path is modeled to represent manual wetwell venting (FL910). Based on user input, a hard-pipe vent line in the wetwell atmosphere may be actuated when containment pressure exceeds 60 psig. This line vents to the environment at an elevation equal to the top of the reactor building. Drywell venting was not modeled in the SOARCA study; however, in the current study two cases of drywell venting were considered. For this, an additional flow path (FL911) was added in the control volume CV201.

Four flow paths (FL901, FL902, FL903, and FL904) represent the flow through various potential breach locations. FL901 represent the torus failure location, FL902 the drywell liner shear, FL903 the head flange leakage, and FL904 the drywell liner melt-through.

The SOARCA wetwell model used a single control volume to represent the hydrodynamic volume in the torus, one downcomer flow path from the lumped vent volume to the wetwell, and one vacuum breaker flow path from the torus airspace back up to the lumped vent volume. While this may have been sufficient to capture the containment pressurization rate for the accident scenarios defined in SOARCA, this same nodalization was found to underpredict the containment pressure for an accident scenario with extended safety relief valve (SRV) cycling and RCIC/HPCI operation as in Unit 3 reactor at the Fukushima Dai-ichi plant where RCIC and SRV discharged steam to the suppression pool for over 20 straight hours.

A refined wetwell model was used for the first set of 15 MELCOR runs for the containment venting issue. The refined model discretizes the torus into 16 equally sized control volumes the sum of which is equal to the original hydrodynamic volume in the PB SOARCA model so the total pool volume is preserved. There is only one volume in the axial direction, and there is still the single lumped vent volume from the SOARCA model. There are 16 interior flow paths connecting each circumferential volume to allow thermal-hydraulic communication between the wetwell volumes. Segmenting the wetwell into smaller circumferential volumes does not treat thermal stratification; nor does it treat wetwell mixing, but it is intended to provide a first-order prediction of asymmetric wetwell heating due to SRV and turbine exhaust.

While the refined model resulted in some improvement in containment pressure prediction, it also added significantly larger computation time for some scenarios and in a few cases, numerical convergence became an issue. For subsequent MELCOR runs, a 2-volume wetwell representation was used but only after checking that the 2-volume representation provided results which are reasonably close to those obtained with a 16-volume representation. Containment structures in the containment model are represented by 23 MELCOR heat structures. Eleven of these heat structures represent the drywell liner-air gap-concrete wall that makes up the boundary between primary and secondary containment (HS10010-HS10020). One drywell liner heat structure is modeled for each reactor building control volume in the reactor building. These rectangular heat structures are made up of carbon steel to represent the drywell liner, an air gap, and a concrete wall. The drywell liner interacts with the drywell control volume, and the concrete wall surface communicates with the appropriate reactor building control volume. The height of these heat structures matches the reactor building control volume in which it resides. Heat structure surface area is calculated so that drywell liner mass is appropriately modeled. Two additional drywell liner heat structures represent the cylindrical (HS10021) and dome (HS10022) portion of the drywell liner within the drywell enclosure. The heat structure film-tracking model is activated to connect film flows between the appropriate drywell liner heat structures.

Eight heat structures are modeled to represent the remaining drywell structures:

- the drywell floor outside of the reactor pedestal (HS10001)
- the drywell floor inside of the reactor pedestal (HS10002)
- the biological shield wall in the lower drywell (HS10003)

- the biological shield wall in the mid-drywell (HS10007)
- the reactor pedestal (HS10004)
- miscellaneous drywell steel in the lower drywell (HS10005)
- miscellaneous drywell steel in the mid-drywell (HS10008)
- miscellaneous horizontal deposition surfaces in the lower drywell (HS10006)

The heat structures representing the drywell floor are modeled as horizontal rectangular heat structures with an insulated boundary condition on one side and the drywell or drywell pedestal region as the other boundary condition. The biological shield wall is split between the lower and mid-drywell volumes as two vertical cylinders that communicate with the drywell at both boundaries. The bottom of the biological shield wall meets the top of the reactor pedestal. The reactor pedestal is represented by a thick vertical cylinder. Drywell miscellaneous steel structures represent equipment within these regions and are modeled by vertical rectangular heat structures.

Miscellaneous horizontal deposition surfaces within the drywell are modeled as upward facing rectangular heat structures with negligible heat capacity (relative to drywell atmosphere) and high thermal conductivity to track drywell temperatures. These heat structures are intended to represent all upward facing fission product deposition surfaces within the drywell (e.g., equipment, cable trays, piping) except for the floor.

Two additional heat structures model the wetwell liner (HS20001) and miscellaneous steel (HS20002). The wetwell liner is modeled as a thick horizontal cylindrical heat structure with a length representing the major torus diameter, and the wetwell (CV220) and main torus room (CV401) as surface boundary conditions. Wetwell miscellaneous steel represents equipment and structures within the wetwell and is modeled by a vertical rectangular heat structure.

Critical pool fractions for heat transfer to the pool and atmosphere are both set at 0.5 for all heat structure surfaces inside primary containment. This allows heat transfer between the heat structure and either the pool or atmosphere, but not both simultaneously. The transition from heat transfer with the pool to heat transfer with the atmosphere occurs when the fraction of the heat structure that is submerged in the pool drops below 0.5. Radiation heat transfer is not modeled for structures within primary containment.

#### **4.6 Reactor Cavity Model**

The drywell floor is subdivided into three regions for the purposes of modeling molten-core/concrete interactions. The first region (which receives core debris exiting the reactor vessel) corresponds to the reactor pedestal and sump floor areas (CAV 0). Debris that accumulates in the pedestal can flow out into the second region (through an open doorway in the pedestal wall), corresponding to a 90 degrees sector of the annular portion of the drywell floor (CAV 1). If sufficient debris accumulates in this region, it can spread further into the third region, which represents the remaining portion of the drywell floor (CAV 2). This discrete representation of debris spreading is illustrated in Figure 5.

Two features of debris relocation within the three cavities are modeled. The first models debris overflow from one cavity to another. The second manages debris spreading radius within the drywell floor region cavities (CAV 1 and 2). Control functions monitor debris elevation and temperature within each region, both of which must satisfy user-defined threshold values for

debris to move from one region to its neighbor. More specifically, when debris in a cavity is at or above the liquidus temperature of concrete, all material that exceeds a predefined elevation above the floor/debris surface in the adjoining cavity is relocated (6 inches for CAV 0 to CAV 1, and 4 inches for CAV 1 to CAV 2). When debris in a cavity is at or below the solidus temperature of concrete, no flow is permitted. Between these two debris temperatures, restricted debris flow is permitted by increasing the required elevation difference in debris between the two cavities (more debris head required to flow).

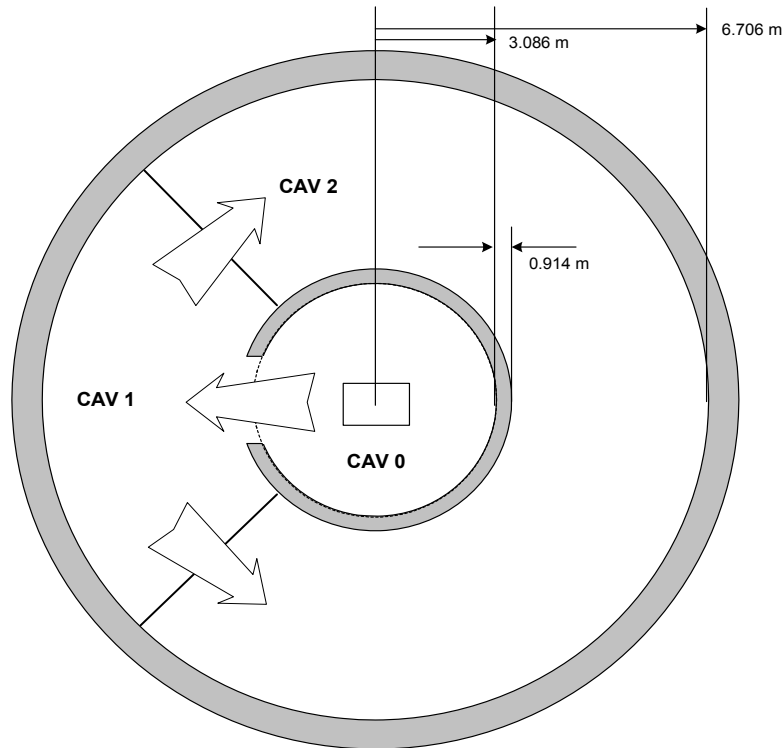


**Figure 5. Discrete representation of debris spreading in the cavity**

Debris entering CAV 1 and CAV 2 are not immediately permitted to cover the entire surface area of the cavity floor. The maximum allowable debris spreading radius is defined as a function of time. When the cavity debris temperature is at or above the liquidus, the shortest transit time (and therefore maximum transit velocity) of the debris front to the cavity wall is determined (10 minutes for CAV 1 as defined in MELCOR control function CF960, and 30 minutes for CAV 2 as defined in control function CF961). When the debris temperature is at or below the solidus, the debris front is assumed to be frozen. A linear interpolation is performed to determine the debris front velocity at temperatures between these two values. The CAVITY package model implemented enforces full mixing of all debris into a single mixed layer.

The solidus and liquidus temperatures in the parametric model that governs the rate of debris spreading on the drywell floor were modified in the present study. Original values of solidus and liquidus temperatures in the PB SOARCA model were 1,420°K and 1,670°K, respectively. These temperatures are representative of concrete solidus and liquidus. For containment

venting calculations, the solidus and liquidus temperatures were changed to 1,700°K and 2,800°K, respectively. The revised liquidus temperature is representative of the liquidus temperature of a eutectic UO<sub>2</sub>/ZrO<sub>2</sub> mixture. The revised solidus temperature was set at 1,700°K to represent the lower bound of average melt temperature at vessel breach, and happens to coincide approximately with the melting point of steel. In the model, spreading is disallowed at debris temperatures less than the solidus temperature and occurs at a maximum rate (0.259 m/min) when debris temperature is above the liquidus temperature. Spreading rate varies linearly at temperatures intermediate between the solidus and liquidus temperatures.

#### **4.7 Balance of Plant Models**

A total of 41 control volumes, 71 flow paths, and 85 heat structures are modeled to represent all pertinent structures external to primary containment. These model elements represent the reactor building, turbine building, radwaste building, and the environment. Given its importance as a fission product release pathway, the reactor building is modeled in significant detail (30 control volumes and 80 heat structures). The turbine and radwaste buildings are considered to have a second order impact on fission product releases to the environment due to the large scale of these buildings and the limited pathways for fission products to enter them. Based on these considerations, the turbine and radwaste buildings are each modeled as single control volumes with one heat structure representing the floor (with the building cross-sectional area) and one nominal leakage flow path. In addition, a single heat structure with surface area equivalent to floor area models horizontal deposition surfaces within the turbine building. The other control volumes external to primary containment represent the reactor building ventilation system (a time-independent control volume fixing reactor building pressure during steady-state conditions), the condensate storage tank (CST), the equipment access lock connected to the reactor building, and the environment.

The reactor building is represented by 30 control volumes. A sectional view of the reactor building is shown in Figure 6. It is modeled on a level-by-level basis, beginning in the basement (i.e., torus room) and sequentially rising up through the main floors to the refueling bay. Control volumes are defined for each region of the reactor building where a volume is deemed to be large in comparison to its flow connectivity areas to other regions of the building. In addition, a finer control volume nodalization is implemented when flow resistances from one building level to another might impact fission product transport (such as in stairwell volumes). When determining the free volume available within control volumes where data on equipment and interior wall displacement are unavailable, it is assumed that 25 percent of the volume calculated based on room dimensions is displaced by these items. For stairwell volumes, it is assumed that 10 percent of the calculated volume is displaced by equipment or walls. For all other reactor building volumes, equipment and miscellaneous displaced volume is either calculated from data (Main Torus Room, Steam Tunnel) or neglected.

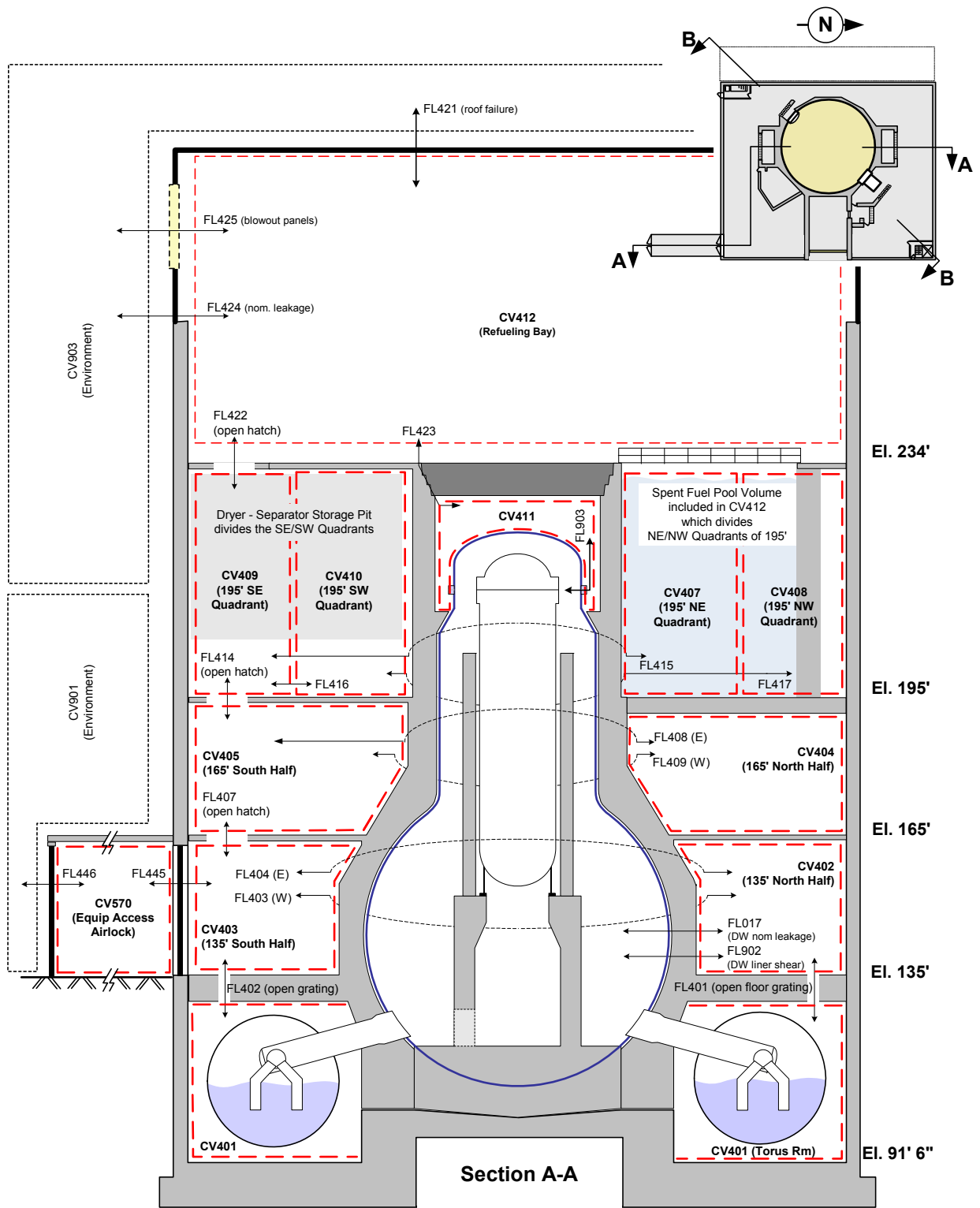


Figure 6. MELCOR nodalization of a sectional view of the reactor building

The torus room level of the reactor building is represented by eight control volumes. These include volumes representing the main torus room, the northeast corner room, the stairwell in the northeast corner of the building, the southeast corner room, and the RHR A, B, C, and D heat exchanger and pump rooms. The next higher level of the reactor building is modeled by five control volumes. These include volumes representing the southern half of the building, the northern half of the building, the southwest stairwell enclosure, the northeast stairwell enclosure, and the steam tunnel. The next higher level of the reactor building is represented by five control volumes. The next higher level of the reactor building is represented by eight control volumes. These volumes represent the northeast, southeast, northwest, and southwest quarters of the floor; the reactor building ventilation room; the drywell enclosure; the southwest stairwell enclosure; and the northeast stairwell enclosure. The refueling bay level (highest level) of the reactor building is represented by four control volumes. These volumes represent the open refueling bay (including the spent fuel pool but neglecting the separator/dryer storage pit), the southwest stairwell enclosure, the northeast corner room and the northeast stairwell enclosure. The 68 flow paths modeled within the reactor building can be classified into the following categories: same level flows between distinct control volumes, open hatches, doors, blowout panels, flow pathways through walls, leakage pathways, stairwells and concrete hatches. Same level flow paths are modeled to connect the distinct control volumes on each floor level (FL403, FL404, FL408, FL409, FL410, FL415, FL416, and FL417). These flow paths are modeled as horizontal. Open hatches connect each of the reactor building levels. Grated hatches exist between the main torus room and both the north and south control volumes (FL401 and FL402). An open hatch pathway exists in the southeast corner of the building to the refueling bay (FL407, FL414, and FL422). Flow paths representing each of these open hatches are modeled as vertical flows with the area of the open hatch.

A total of 25 flow paths are modeled representing doors within the reactor building. Both double and single door characteristics are modeled. Each flow path representing a single-style door is modeled as a horizontal flow. Each door has a combination of a valve and control functions to model door failure based on building overpressures. Each double door is assumed to be leaktight under nominal conditions, but has a combination of a valve and control functions to model door failure based on building overpressures.

Three flow paths are modeled representing blowout panels within the reactor building. Each of these is represented as a horizontal flow path with a valve and control function logic managing open fraction. Ten flow paths are modeled to represent open pipe chases and fire dampers through walls or floors (FL430-FL435, FL437, FL443-FL444, and FL451). Two flow paths are modeled to represent leak-type pathways. FL424 is a horizontal pathway representing nominal leakage through the refueling bay walls and ceiling. FL423 is a vertical pathway representing the leakage from the drywell enclosure through the concrete plug gap to the refueling bay. Seven flow paths represent vertical flows through the southwest (FL482, FL484, and FL486) and northeast stairwells (FL462, FL465, FL470, and FL474) in the reactor building. Six vertical flow paths represent concrete hatches that may be displaced by building overpressures. One additional reactor building flow path (FL450) connects the reactor building ventilation system (CV450) with the northern half of the reactor building. Nominal reactor building leakage occurs through the refueling bay walls/ceiling and closed doorways connecting the reactor building to the environment, turbine building, and radwaste building.

Structures within the reactor building are represented by 83 MELCOR heat structures. These heat structures can be classified in one of the following categories: floor/ceiling, exterior walls,

interior walls, horizontal fission product deposition surfaces, or miscellaneous steel. Each reactor building control volume representing part of the primary room at each building level (CV401-410, 412) is modeled with heat structures representing the room's floor, ceiling, exterior walls, and miscellaneous steel. Each of these control volumes, excluding the refueling bay, also contains a heat structure representing internal walls. Each room floor is modeled as a horizontal slab with a surface area equal to the projected area of the room. For floors between two building levels, a two-sided heat structure represents the floor for the upper volume and the ceiling for the lower volume.

Exterior concrete walls are modeled as vertical slabs with an adiabatic boundary condition on the outside surface (due to interfaces with multiple external volumes and assumption that concrete wall thickness allows adiabatic assumption). Miscellaneous steel and internal walls are both modeled as rectangular-vertical heat structures. Internal walls within these volumes represent spent fuel pool walls, the separator/dryer storage pit walls, or miscellaneous structures. Miscellaneous steel represents equipment located within each volume. Miscellaneous internal wall structures and steel are modeled with model legacy values.

Horizontal fission product deposition surfaces within the reactor building are modeled as upward facing rectangular heat structures with negligible heat capacity (relative to drywell atmosphere) and high thermal conductivity to track drywell temperatures. This heat structure is intended to represent all upward facing fission product deposition surfaces (e.g., equipment, cable trays, piping) located in a particular region of the building (with the exception of the floor). Since fission product releases may occur at higher elevations in the reactor building (via drywell liner penetration shear, interfacing-systems loss-of-coolant-accident breaks), horizontal fission product deposition surfaces are modeled at these reactor building levels. Additional horizontal deposition surface area within these regions was estimated as projected floor area.

Rooms modeled within the reactor building that are accessible only via doorways are considered of secondary importance to fission product distribution. For these control volumes (CV452-458, 460), modeling of heat structures is limited to a slab representing projected floor area and steel representing grated floors in the RHR heat exchanger and pump rooms. Stairwell control volumes are only accessible via initially closed doorways, and heat structure modeling for these spaces is limited to a slab representing projected floor area and steel representing the stairwell structures.

## 5. MELCOR CALCULATIONS FOR CONTAINMENT FILTERED VENTING SYSTEM ANALYSIS

In developing the MELCOR calculation matrix for containment filtered venting system analysis, a set of accident prevention and mitigation measures were considered, informed by the lessons learned from the Fukushima event, accident management alternatives contemplated by the industry, the current state of knowledge of severe accident progression in a BWR and mitigation alternatives, and by the experience gained from the SOARCA study. The accident scenarios considered are both long-term and short-term station blackout (SBO) leading to one of three possible outcomes: containment overpressure failure, liner melt-through failure, or maintaining the containment intact as a result of venting or other mitigation measures.

In a SBO with the loss of all cooling function and absent any mitigation measures, the core is going to uncover leading to heatup, degradation, relocation of degraded core into lower plenum, thermal loading of the reactor pressure vessel (RPV) lower head and consequent lower head failure, relocation of core debris into the reactor cavity, and ultimate containment failure by overpressure or other mechanisms. It is assumed that low-pressure core injection (LPCI), high-pressure core injection (HPCI), drywell spray, and other engineered safety features (ESF), normally designed to run by AC power, become unavailable for an extended period of time.

For this type of situation, the reactor core isolation cooling (RCIC) system is designed to provide core cooling, thus delaying core uncover and subsequent accident progression until such time other DC-powered (battery or diesel generator) and portable mitigation systems become available. The RCIC operation is controlled by battery, which acts as a power source for control valves that run the RCIC pump on and off. Before battery depletion, the RCIC is throttled to maintain a nominal RPV water level. In the SOARCA model, the RCIC continues operating after battery depletion, albeit in a "locked" state (i.e., without throttling). Cooling of the core by RCIC continues during this period.

The operation of RCIC was considered as the first preventative/mitigative feature in developing the MELCOR calculation matrix. For most MELCOR cases documented in this report, core cooling by RCIC continues for 2 hours or so after battery depletion until the main steam lines are flooded. In a few cases, the RCIC operation was specified so as not to have an additional period of core cooling from steam line flooding.

The SOARCA study assumed RCIC operation for 4 hours. Many, if not most, BWR Mark I plants are equipped with batteries that will allow RCIC to run for an extended period of as much as 8 hours. Moreover, in the post-911 development of accident management strategies, conceivably even a longer battery life for RCIC operation may have been considered. In Fukushima Dai-ichi Unit 2, RCIC operation in excess of 70 hours has been reported although the reason for such an extended operation is yet unknown. Likewise, in Fukushima Dai-ichi Unit 3, RCIC operation on the order of 20 hours has been reported, followed by another 16 hours of HPCI operation that kept the core cooled. With these considerations in mind, RCIC operation of 16 hours has been assumed in most of the MELCOR calculations reported here. For sensitivity analysis, one calculation with RCIC operation time of 4 hours (so the results can be compared with the SOARCA results) and a limited number of calculations with RCIC operation time of 8 hours were also performed. Also, a calculation was performed with RCIC failing to start, simulating a short-term SBO scenario.

Upon termination of RCIC operation, the next mitigation feature considered in the current study is actuation of core spray. As it is not clear at this time that the HPCI system can be actuated with portable devices, a diesel generator driven fire water system was considered to feed the low-pressure core spray system but only after RPV depressurization. A 300 gpm flow rate for the core spray was used in the analysis.

Another mitigation feature considered in the current study is drywell spray with a nominal flow rate of 300 gpm. As in the case of core spray, the drywell spray is assumed to be operated by a diesel-powered portable device. The drywell spray is actuated at 24 hours which, in most cases, correspond to the timing of RPV lower head failure. Variation in drywell spray actuation time was considered as part of the sensitivity study.

In addition to the mitigation features above, containment venting was considered in the current study in a number of ways. The primary function of venting is to prevent containment failure by overpressure from steam and other noncondensable gases. The BWR Mark I plants were originally designed with wetwell vents that had a low pressure capacity. As a result of post-TMI improvements, the wetwell vents in many of these plants have been upgraded and “hardened” for a high pressure capacity. Nevertheless, the vents were not designed or upgraded for operation under severe accident conditions. Core degradation and consequent hydrogen generation from steam oxidation of the degraded core and other core structures will add to containment loading resulting in containment overpressurization. In this situation, venting will prevent containment failure by overpressure, and greatly reduce the hydrogen, steam, and radioactive airborne contamination leaking into the secondary containment which could have resulted in a high dose environment, thus impeding accident mitigation and recovery actions by the operators. However, venting will also create a leakage path for fission products to escape to the environment, thus increasing health and land contamination risk. For these reasons, venting alone is not considered an adequate accident management measure; rather, venting in combination with other mitigation features is considered for further investigation in the current study. In all cases where venting is considered, it is initiated at a pressure of 60 psig.

Venting through the wetwell has the advantage of attenuating fission products through suppression pool scrubbing. Generally speaking, the fission products or aerosol particle size distribution is altered through the suppression pool scrubbing process as shown in Figure 7 below for a 300 cm deep pool and representative accident conditions. This figure illustrates the aerosol removal efficiency being highly dependent on particle size. The probability distributions in the figure are mass weighted and normalized to the total mass input to the pool. The dashed portion of the input size distribution curve (green) in the figure denotes large particles ( $>10\ \mu\text{m}$ ) that are typically deposited in transport and do not actually reach the suppression pool. Particles larger than  $1\ \mu\text{m}$  are efficiently removed by gravitational settling or inertial impaction. Very small particles ( $<0.1\ \mu\text{m}$ ) are removed by the diffusion process. Particles of intermediate size are removed by interception with the bubble in the suppression pool. When all removal mechanisms are considered, the efficiency of removal passes through a minimum when plotted against particle size. The particle size corresponding to the minimum efficiency (correspondingly known as the “maximum penetration size”) is around  $0.2\ \mu\text{m}$ . The difference in removal efficiency between the larger particles and the maximum penetration size particles can be two orders of magnitude or more.

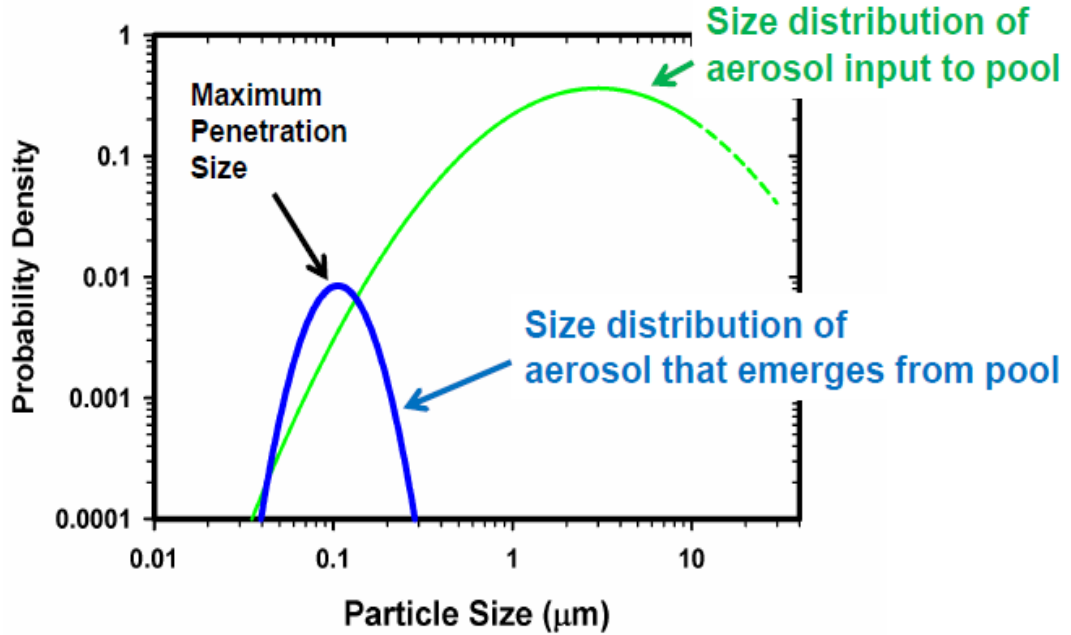


**Figure 7. Aerosol removal efficiency as a function of particle size**

Decontamination from pool scrubbing both attenuates the amount of mass and narrows the size distribution so the altered size distribution (blue) is centered around the maximum penetration size. Additional decontamination may result from adding a filter on the vent line. The effectiveness of the filter at the wetwell end varies depending on the filter design and construction. The altered particle size distribution emerging from the suppression pool is not nearly as amenable to further decontamination by a filter of the traditional variety. More recent filtration technology appears to provide a DF far in excess of the somewhat low range of DF achievable by traditional filters. Note the suppression pool itself has a DF calculated internally within the SPARC90 module of the MELCOR code, which was benchmarked against the Electric Power Research Institute (EPRI)-sponsored Advanced Containment Experiment (ACE) data [11] and Battelle Columbus Laboratories experiments [12]. The combined DF (i.e., suppression pool and wetwell filter) can be quite significant.

In the current MELCOR analysis, the calculated suppression pool DF varies from nominally 100 to 300 depending on the pool depth, pool temperature, and other factors. This range of calculated DF is bounded by the estimated pool DF (see Figure 8), which has a much larger variation and correspondingly, large uncertainties [13]. Also, in the current MELCOR analysis, a DF in the range of 2 to 10 is assumed for the wetwell filter instead of a DF of 1,000 or more that the currently available filtration technology can provide. This assumption is predicated upon the fact that the aerosol size distribution is altered after going through the pool scrubbing process, and the altered size distribution is not nearly as amenable to high decontamination as the original size distribution would be.

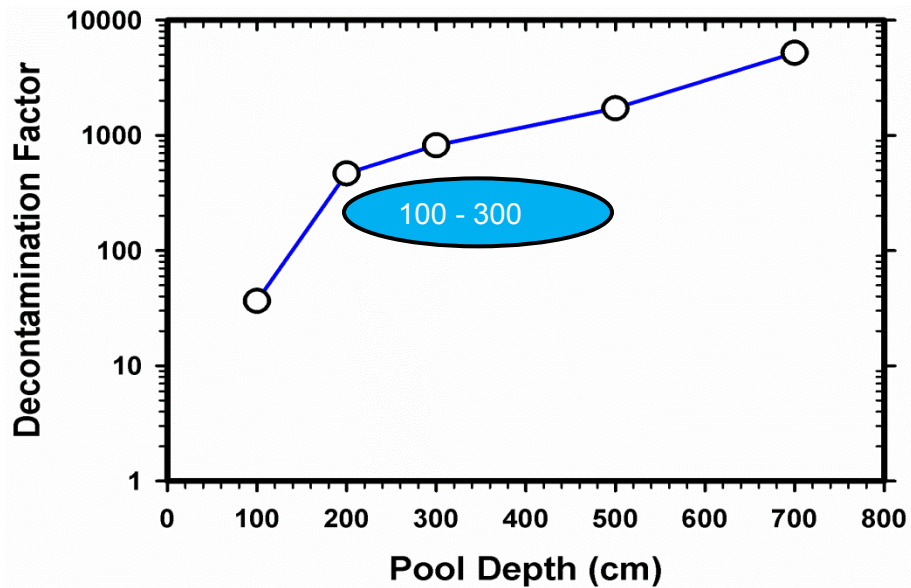


**Figure 8. Estimated decontamination factor as a function of pool depth**

The BWR Emergency Procedure Guidelines, which form the basis for plant specific emergency operating procedures, contain provisions for containment venting through the wetwell and drywell. Some BWR Mark I plants have drywell vents in addition to wetwell vents. In those plant configurations where the wetwell vent path is blocked (e.g., high suppression pool level), drywell venting essentially serves the same purpose as the wetwell venting in most designs. The drywell venting does not have the benefit of suppression pool scrubbing upstream of the vent. However, since the fission product aerosols are not scrubbed by the pool after reactor vessel breach, they retain their original size distribution by and large and are, therefore, amenable to significant attenuation by a filter at the drywell end. As a variation to wetwell venting, the current analysis considered two cases of drywell venting for comparison.

A large number of MELCOR cases were run for the containment venting study as described below. Most of the cases represent long-term SBO as in the Fukushima event and the SOARCA studies. Also, these cases consider RCIC operation and a combination of one or more mitigation features such as core spray, containment spray, and venting. The cases with venting include the option of wetwell (majority of the cases) and drywell venting (two cases). Collectively, the MELCOR cases provide all representative combinations of prevention and mitigations measures which are considered in the description of options used in the regulatory analysis (Enclosure 1). The MELCOR cases are summarized below in Table 3.

MELCOR does not model the effect of an external filter on fission product releases. This effect is considered in the MACCS analysis through the use of a prescribed DF value. In other words, in those cases where venting is present, release fractions calculated by MELCOR are used to perform two sets of MACCS calculations—one using the prescribed filter DF and the other as the unfiltered case. The comparison between the filtered case and the unfiltered case provides an indication of the effectiveness of filter.

**Table 3. Matrix of MELCOR Cases for Containment Venting Study**

MELCOR Case Description	Case 1	Case 2	Case 3	Case 4	Case 5	Case 6	Case 7	Case 8	Case 9	Case 10
RCIC with 4-hour battery life	X									
RCIC with 8-hour battery life								X	X	X
RCIC with 16-hour battery life		X	X	X	X	X	X			
16-hour extended RCIC operation with 8-hour battery life										
Wetwell venting at 60 psig, vent open			X				X		X	
Wetwell vent cycled, open at 60 psig and close at 45 psig				X						
Drywell venting at 24 hours										
Core spray after RPV lower head failure						X	X			X
Drywell spray at 24 hours										
Drywell spray at 16 hours										
Drywell spray at 8 hours										
SRV stuck-open mechanism disabled—MSL creep rupture										
Traveling in-core probe leak to containment										
SRV seal leakage										
Short term SBO with RCIC failure to start										

Notes:

- Case 5 is a variation of Case 2 where the CST inventory is reduced to half its volume to determine the sensitivity. Makeup water for RCIC operation is provided from the CST until it is empty. After that, suction is taken from the suppression pool.
- Core spray flow rate is 300 gallons per minute (gpm) for Cases 6, 7, and 10.

**Table 3. Matrix of MELCOR Cases for Containment Venting Study (continued)**

MELCOR Case Description	Case 11	Case 12	Case 13	Case 14	Case 15	Case 16	Case 17	Case 18	Case 19	Case 20
RCIC with 4-hour battery life										
RCIC with 8-hour battery life	X									
RCIC with 16-hour battery life		X	X	X	X					
16-hour extended RCIC operation with 8-hour battery life						X	X	X	X	X
Wetwell venting at 60 psig, vent open	X									
Wetwell vent cycled, open at 60 psig and close at 45 psig					X					
Drywell venting at 24 hours		X	X							
Core spray after RPV lower head failure	X									
Drywell spray at 24 hours			X	X	X					X
Drywell spray at 16 hours									X	
Drywell spray at 8 hours								X		
SRV stuck-open mechanism disabled —MSL creep rupture		X	X							
Traveling in-core probe leak to containment										
SRV seal leakage										
Short term SBO with RCIC failure to start										

Notes:

- Drywell spray flow rate is 300 gpm for cases 13, 14, 15, 18, 19, and 20. Variations of flow rate considered in sensitivity analysis (Cases 28 through 30).
- Cases 16 through 25 were run with 2-volume wetwell nodalization in contrast to Cases 1 through 15, which were run with 16-volume nodalization. Two-volume nodalization provided improved computational efficiency.

**Table 3. Matrix of MELCOR Cases for Containment Venting Study (continued)**

MELCOR Case Description	Case 21	Case 22	Case 23	Case 24	Case 25	Case 26	Case 27	Case 28	Case 29	Case 30
RCIC with 4-hour battery life										
RCIC with 8-hour battery life										
RCIC with 16-hour battery life						X		X	X	X
16-hour extended RCIC operation with 8-hour battery life	X	X	X	X	X		X			
Wetwell venting at 60 psig, vent open	X	X	X	X	X			X	X	X
Wetwell vent cycled, open at 60 psig and close at 45 psig						X	X			
Drywell venting at 24 hours										
Core spray after RPV lower head failure										
Drywell spray at 24 hours								X	X	X
Drywell spray at 16 hours										
Drywell spray at 8 hours	X	X	X	X	X	X	X			
SRV stuck-open mechanism disabled —MSL creep rupture		X								
Traveling in-core probe leak to containment			X							
SRV seal leakage				X						
Short term SBO with RCIC failure to start					X					

Notes:

- Case 28 is variation of Case 14 with 100 gpm drywell flow rate, Case 29 is variation with 500 gpm flow rate, and Case 30 is variation with 1,000 gpm flow rate.

Cases 2, 3, 6, 7, 12, 13, 14, and 15 are selected as MELCOR base cases, the results of which are used for MACCS consequence calculations and for regulatory analysis. The rest of the cases were run as variations of the base cases for sensitivity analyses. The base cases represent no venting or spray (Case 2), wetwell venting but no spray (Case 3), core spray only (Case 6), core spray with wetwell venting (Case 7), drywell venting (Case 12), drywell venting and drywell spray (Case 13), drywell spray only (Case 14) and drywell spray with wetwell venting (Case 15). Collectively, the base cases provide all representative combinations of prevention and mitigations measures which are considered in the description of options used in the regulatory analysis (Enclosure 1). For example, Case 2 with no venting or spray maps to Option 1 (status quo) in the regulatory analysis. Likewise, all venting cases (Cases 3, 7, 12, 13, and 15) map to Option 2 (severe accident capable vent) and, when considered in combination with an external filter, to Option 3 (filtered vent). Case 6 and Case 14 (both nonventing but with sprays) may be considered variations of Option 1. Note the base cases are similar to the cases used in EPRI's analysis mentioned before with one exception. EPRI considered cycled venting as a mitigation strategy in its analysis. The MELCOR base cases do not include cycled venting; however, this mitigation feature was considered as part of additional MELCOR sensitivity analysis. As discussed later, MELCOR analysis did not find any significant differences between cycled venting cases and once-open venting cases with regard to fission product release estimates.

All the base cases assumed RCIC operation with 16-hour battery life. Each calculation was terminated after 48 hours of transients, consistent with the SOARCA study and based on observations therein that fission product releases occur mostly in the first 48 hours. MELCOR calculations and the results are discussed in detail below. Table 4 shows the timing of key events and MELCOR results for selected base cases. A discussion of the sensitivity cases and their results is provided following the discussion of the base cases.

### **5.1 Case 2 (No Venting or Spray)**

Case 2 represents a long-term SBO situation resulting in the loss of all cooling functions. RCIC is operational by battery power with a mission time of 16 hours. The RCIC flow terminates at about 18 hours after SBO (additional 2 hours after depletion of battery). The core is subsequently uncovered at about 23 hours after SBO. Core oxidation starts shortly thereafter, resulting in hydrogen production. In the meantime, core degradation proceeds, resulting in core relocation to the lower head and subsequent lower head dryout at about 30 hours. The thermal loading of the lower head at this time and forward ultimately leads to its gross failure at about 37 hours.

Since this case does not allow any venting, the pressure from steam and noncondensable builds up in the containment leading to drywell head flange leakage at a pressure exceeding its design limit of 80 psig. (This assumed leakage scenario is based on the information available and analysis performed on Fukushima Dai-ichi Unit 1.) The leakage starts long before the RPV lower head failure. With the leakage path created, any pressure buildup in excess of 80 psig due to continued noncondensable production is relieved, and the drywell pressure remains at the design limit until the failure of the lower head by thermal loading.

**Table 4. Matrix of MELCOR Calculations Showing Timing of Key Events**

Event Timing (hr.)	Case 2 (no venting)	Case 3 (wetwell venting)	Case 6 (core spray)	Case 7 (core spray + wetwell venting)
Station blackout	0.0	0.0	0.0	0.0
RCIC flow terminates	17.9	17.9	17.9	18.0
Active fuel uncover	22.9	22.9	22.9	22.9
First hydrogen production	23.6	23.6	23.6	23.2
Relocation of core debris to lower plenum	25.9	25.9	25.9	25.8
RPV lower head dries out	30.3	28.6	29.6	28.1
RPV lower head fails grossly	37.3	34.3	36.7	33.8
Drywell pressure > 60 psig—vent opens if applicable	22.8	22.8	23.3	23.2
SRV sticks open	22.7	22.7	22.7	22.7
Drywell head flange leakage (>80 psig)—overpressure failure	25.5	---	25.4	---
Drywell liner melt-through	40.3	36.6	---	---
Calculation terminated	48	48	48	48
<b>Selected MELCOR Results</b>	<b>Case 2</b>	<b>Case 3</b>	<b>Case 6</b>	<b>Case 7</b>
Debris mass ejected (1,000 kg)	286	270	255	302
In-vessel hydrogen generated (kg-mole)	525	600	500	600
Ex-vessel hydrogen generated (kg-mole)	461	708	276	333
Other noncondensable generated (kg-mole)	541	845	323	390
Iodine release fraction at 48 hrs	2.00E-02	2.81E-02	1.70E-02	2.37E-02
Cesium release fraction at 48 hrs	1.32E-02	4.59E-03	3.76E-03	3.40E-03

At lower head failure, the molten core debris relocates to the drywell cavity and spreads to the cavity perimeter and to the drywell liner. The thermal loading imparted on the liner by core debris challenges the liner integrity and the liner ultimately breaches by melt-through at about 40 hours or about 3 hours after the RPV failure. Core-concrete interactions, initiated due to molten core relocation to the drywell floor, generate noncondensable gases and fission product aerosols. These fission products along with those generated in-core are released to the environment at liner melt-through and the release is not scrubbed or filtered as the release path bypasses the wetwell.

**Table 4. Matrix of MELCOR Calculations Showing Timing of Key Events (continued)**

Event Timing (hr.)	Case 12 (drywell venting)	Case 13 (drywell venting + drywell spray)	Case 14 (drywell spray)	Case 15 (drywell spray + wetwell venting)
Station blackout	0.0	0.0	0.0	0.0
RCIC flow terminates	17.9	17.9	17.9	18.0
Active fuel uncover	24.0	24.0	22.9	22.9
First hydrogen production	24.3	25.0	23.2	23.2
Relocation of core debris to lower plenum	28.3	28.7	25.7	25.6
RPV lower head dries out	28.9	29.1	29.4	29.3
RPV lower head fails grossly	34.2	34.7	36.6	35.3
Drywell pressure > 60 psig—vent opens if applicable	27.7	27.7	23.2	23.3
SRV sticks open	27.2	27.3	22.7	22.4
Drywell head flange leakage (>80 psig)—overpressure failure	27.6	---	35.2	---
Drywell liner melt-through	34.8	35.1	---	---
Calculation terminated	48	48	48	48
<b>Selected MELCOR Results</b>	<b>Case 12</b>	<b>Case 13</b>	<b>Case 14</b>	<b>Case 15</b>
Debris mass ejected (1,000 kg)	345	351	267	257
In-vessel hydrogen generated (kg-mole)	670	750	614	650
Ex-vessel hydrogen generated (kg-mole)	774	410	327	276
Other noncondensable generated (kg-mole)	922	485	383	270
Iodine release fraction at 48 hrs	4.90E-01	4.84E-01	5.41E-03	1.86E-02
Cesium release fraction at 48 hrs	1.93E-01	1.86E-01	1.12E-03	3.01E-03

## 5.2 Case 3 (Wetwell Venting)

Case 3 is basically identical to Case 2, but this time venting is in effect. The wetwell vent opens at about 23 hours after SBO when the drywell pressure exceeds 60 psig and remains open. This prevents containment failure by overpressure. However, as in Case 2, at lower head failure, the relocated core debris on the drywell floor spreads to the liner, and attacks the same leading to melt-through and containment breach. Also, as in Case 2, fission products are released to the environment at liner melt-through and this release is not scrubbed or filtered as the release path bypasses the wetwell. However, any release through wetwell vent prior to liner melt-through (a duration of about 14 hours between vent opening and liner melt-through timing) is scrubbed efficiently by the suppression pool.

## 5.3 Case 6 (Core Sprays)

Case 6 examines the mitigation effect of core spray. In the present study, it is assumed that the core spray can only be actuated at a sufficiently low pressure when using a hookup from a portable fire-water system. Specifically, it is assumed that the core spray system is actuated at

reactor vessel failure, which depressurizes the vessel. Moreover, it is assumed that a nominal flow rate of 300 gpm is achievable using a portable system. With the core spray actuation at vessel breach, water finds its way to the drywell floor. The net effect is slowing down of core debris spreading on the floor to the point of effectively freezing the debris, thus arresting further progression. As a result, the liner melt-through is prevented. However, since this case does not involve any venting, the drywell pressure builds up, leading eventually to containment overpressure failure (through head flange leakage).

#### **5.4 Case 7 (Core Sprays and Wetwell Venting)**

Case 7 builds on Case 6 by adding wetwell venting. As in Case 6, actuation of core spray at vessel breach using a fire water system at 300 gpm flow rate provides water to the drywell floor. The net effect is slowing down of core debris spreading and prevention of liner melt-through. Any fission product release, in this case, goes through wetwell vent and in the process, gets scrubbed by the suppression pool.

Case 7 may be contrasted with Case 6 as well as the two previous cases (Case 2 and Case 3) with no spray action. Case 6 examines the effect of core spray only with no venting in effect. While the absence of venting in Case 6 leads to containment overpressure failure by drywell head flange leakage as in Case 2, actuation of core spray has a scrubbing effect on in-core fission products. As a result, the total amount of fission products released in Case 6 is smaller than those for both Case 2 and Case 3. Case 7 examines the combined effect of core sprays and venting. The combined effect shows smaller release amounts in Case 7 than those in Case 2 and Case 3, and similar releases compared to Case 6.

#### **5.5 Case 12 (Drywell Venting)**

Case 12 explores the efficacy of drywell venting with an external filter downstream of the vent. In Case 12 (also in Case 13 discussed later), the SRV sticking mechanism was disabled and the wetwell vent was assumed closed. This is to simulate a transport path of steam, noncondensable gases, and fission products through the drywell vent.

Some BWR Mark I plants implemented a severe accident management strategy whereby the reactor cavity is flooded above the wetwell vents making wetwell venting inoperable. Some Mark I plants in the United States are equipped with both drywell and wetwell vents and depending on the accident sequences and failure modes, either or both may be operable. Any fission products released through a drywell vent will not be scrubbed at all unless there is a filter. By the same token, fission products passing through a filtered drywell vent will be greatly attenuated since the size distribution of fission product aerosols is amenable to a high degree of decontamination.

Case 12 is simulated in MELCOR in a manner that is similar to a main steam line rupture scenario considered for the Fukushima Dai-ichi Unit 1. The MELCOR analysis of Unit 1 shows that core exit gas temperatures began to significantly increase, with superheated steam and hydrogen gas flowing into the main steam line associated with the cycling SRV (achieved in MELCOR by disabling SRV sticking open mechanism). This hot gas heated the steam line significantly, and because the reactor pressure was high (at the lowest SRV set point), thermal creep in the hottest steam line eventually led to failure of the main steam line and resulting depressurization of the RPV. The loss of pressure boundary in this mode is believed to be consistent with the data from Fukushima Dai-ichi Unit 1.

## **5.6 Case 13 (Drywell Venting and Drywell Sprays)**

Case 13 builds on Case 12 by adding a drywell spray operation initiated at 24 hours. As in Case 12, the SRV sticking mechanism is disabled and the wetwell vent is closed to simulate the transport path of fission products through the drywell vent. Also, as in Case 12, this case is simulated in MELCOR in a manner that is similar to a main steam line rupture scenario.

A nominal 300 gpm drywell spray flow rate was assumed in this scenario. This rate is an order of magnitude less than the design-basis flow rate of the installed drywell spray header. However, this nominal flow rate is considered reasonable when a portable or diesel operated device is used in an SBO. It is anticipated that the sprays would provide the benefits of washing some fraction of the fission product aerosols from the drywell atmosphere, thus making them unavailable for release to the environment.

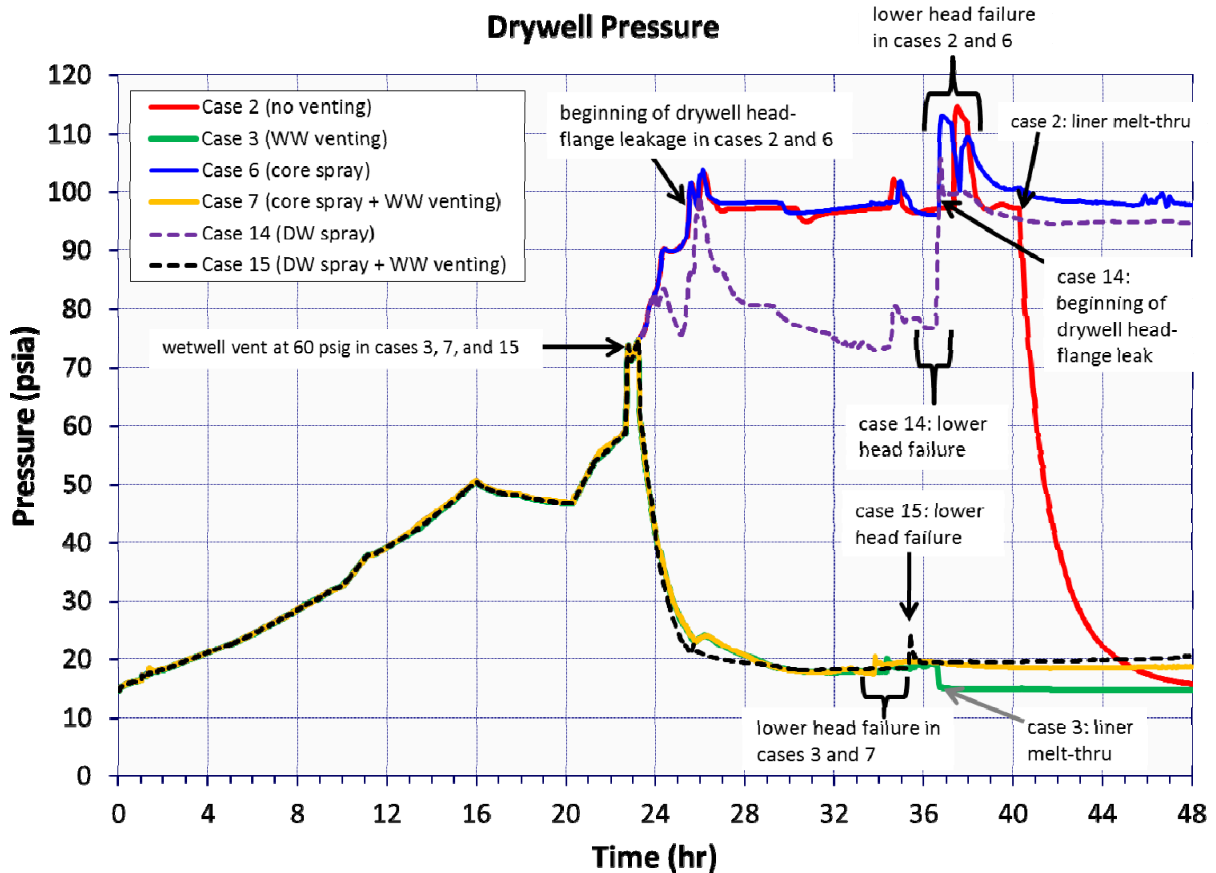
## **5.7 Case 14 (Drywell Sprays)**

Case 14 explores the effect of drywell sprays which differ from core sprays (Case 6) in terms of their influence on containment pressure and aerosol washoff. Sprays with a flow rate of 300 gpm are actuated at 24 hours (about 2 hours before the drywell head flange leakage and more than 12 hours before the lower head failure). Since there is no vent opening, the case results in containment failure by overpressure. Fission products, leaked through the head flange leakage path, are scrubbed to some degree by the drywell spray action, which reduces the release to the environment. Likewise, fission products released after vessel failure are scrubbed by the spray.

## **5.8 Case 15 (Drywell Sprays and Wetwell Venting)**

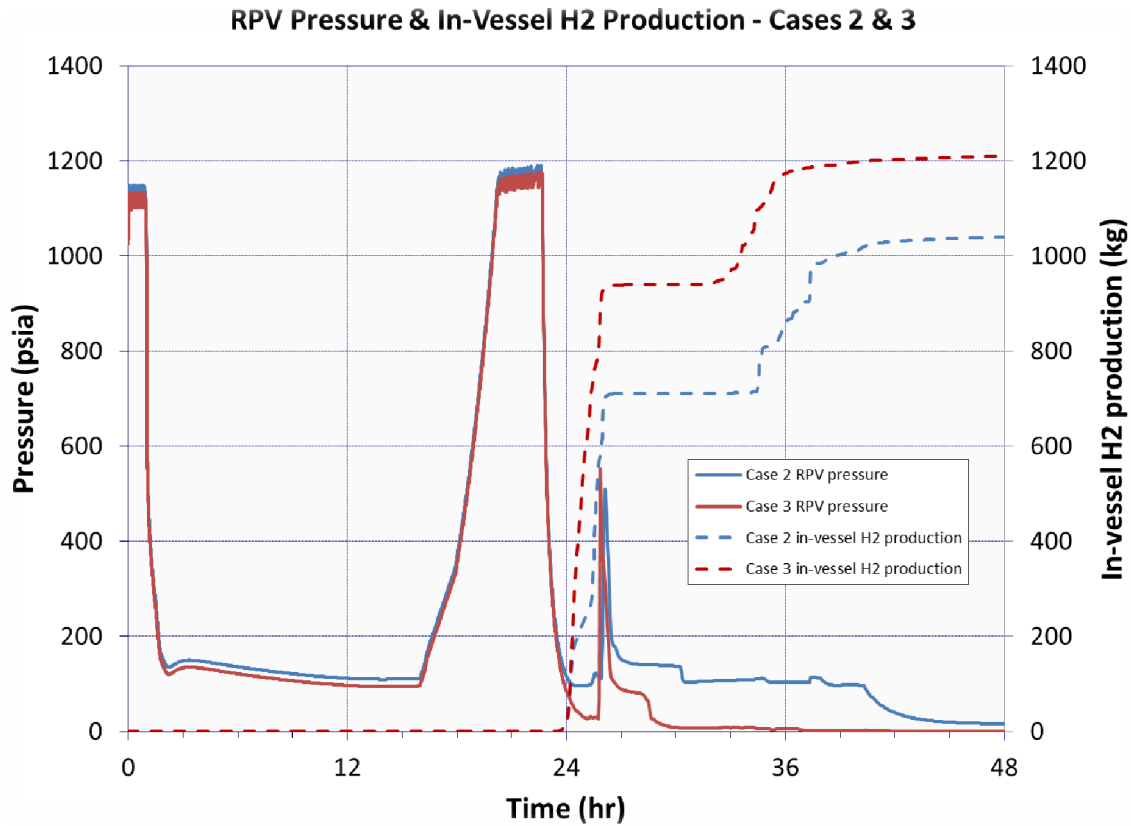
Case 15 is a variation of Case 14 in which wetwell venting is added. This action prevents containment overpressure failure. The RPV lower head fails in this case at about 35 hours (as opposed to 36 hours for Case 14), whereas the containment spray starts at 24 hours (same as in Case 14). The spray action creates a pool of water in the cavity and in the pedestal region. At vessel failure when the fission products are released, the pool of water provides some scrubbing effect. Further, as the fission products are released through the wetwell vent to the environment, additional scrubbing by the suppression pool takes place. The combined effect of the two scrubbing processes is significant, resulting in a smaller release to the environment.

Figure 9 shows a comparison of drywell pressure for six cases, three of which are not vented (Cases 2, 6, and 14) and the other three (Cases 3, 7, and 15) vented through the wetwell. As seen in this figure, both Case 2 and Case 3 lead to liner melt-through since there is no provision of water in these two cases to cool the core debris and prevent melt spreading to the liner. Case 7 and Case 14, on the other hand, have provision for water as do Case 6 and Case 15. Of these latter four cases, Case 6 and Case 14 do not have venting. As a result, these two cases lead to containment failure by overpressure, indicated in the figure by drywell head flange leakage. Case 2 also has no venting and hence, leads to overpressure failure. It is interesting to note that the drywell spray action in Case 14 relieves the containment pressure for a while and delays the overpressure failure by over 10 hours (~25 hours in Case 6 versus ~37 hours in Case 14). It is also interesting to note that in Case 14, gross failure of the RPV lower head precedes the head flange leakage, though not by much, whereas in Case 2 and Case 6, the lower head fails much later. Cases 3, 7, and 15 all have venting which prevents containment overpressure failure.



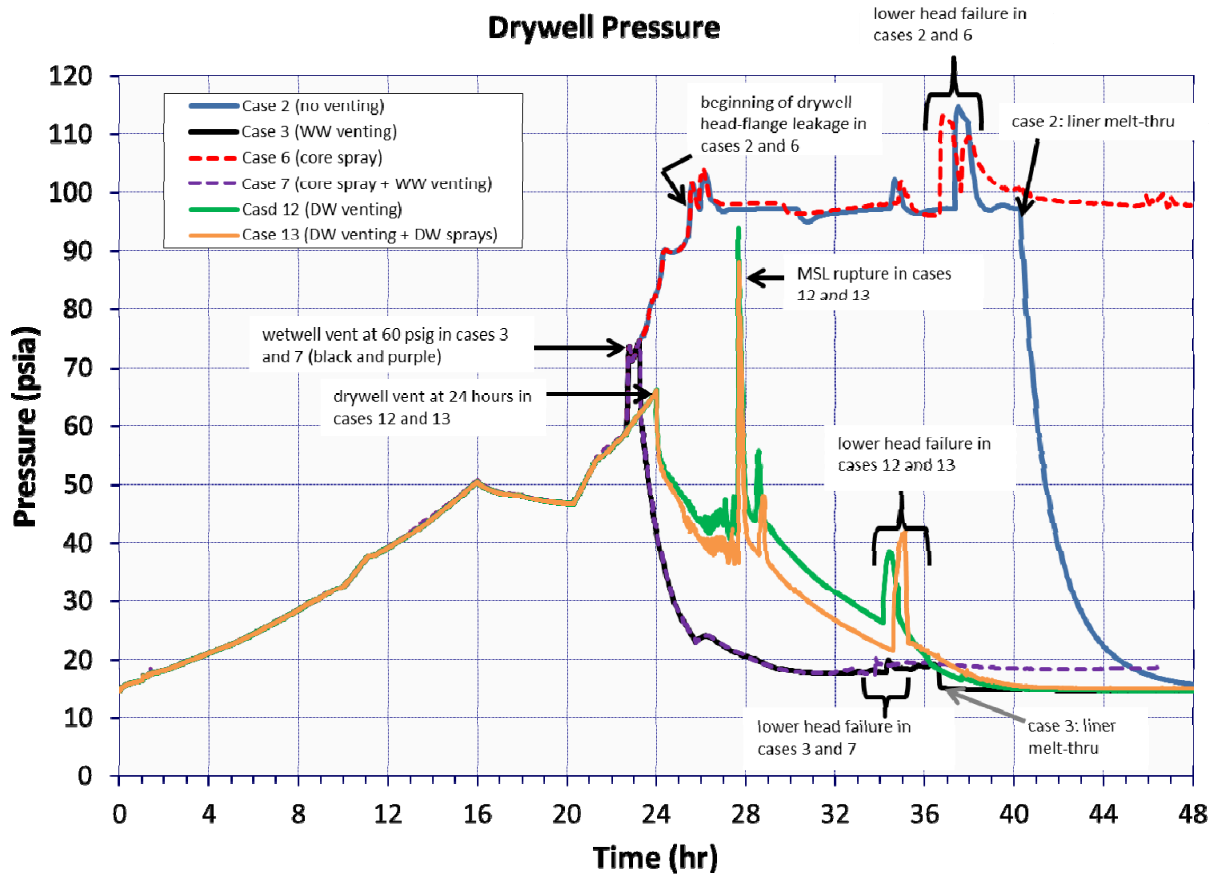
**Figure 9. Comparison of drywell pressures for selected cases**

Figure 9 also indicates that in all venting cases, the lower head failure occurs earlier than in nonventing cases (by about 2 to 3 hours). It is important to note the degree of core oxidation strongly affects the timing of lower head failure and that oxidation is steam limited at times. Steam evolves largely from the boiling of water in the reactor lower plenum but not entirely. It also evolves from flashing liquid as the reactor depressurizes. The rate of depressurization governs the rate that steam via flashing. As long as choked flow persists in the SRV (the lowest set-point SRV) reactor pressure is not responsive to containment pressure. However, choked flow will abate at some point as the reactor depressurizes through a failed (stuck-open) SRV. Once choked flow through the SRV abates, containment pressure influences reactor pressure and hence steam evolution from flashing. Lower containment pressures relate to lower reactor pressure and more flashing. The LTSBO cases where the containment is vented with the vent left open lead to very low containment pressures and hence, more steam production from flashing, lower reactor pressure, more oxidation, and hydrogen generation seen in Figure 10 below. Finally, increased oxidation leads to hotter debris relocated to the lower plenum and earlier lower head failure.



**Figure 10. Comparison of RPV pressure and in-vessel hydrogen production in Cases 2 and 3**

Figure 11 shows another comparison of drywell pressure for six cases—this time two of the venting cases involve drywell venting (Cases 12 and 13) and the other four are Cases 2, 3, 6, and 7 as before.



**Figure 11. Comparison of drywell pressures for selected cases highlighting drywell venting**

Disabling the SRV failure mechanisms in Cases 12 and 13 led to main steam line creep rupture as seen in Figure 11. Generally, in the LTSBO calculations, developing a pool on the containment floor prior to reactor lower head failure allowed core debris to quench to the point that it could not migrate to the drywell liner and hence could not melt through the liner. In Case 13, however, disabling the SRV failure mechanisms led to more core degradation occurring at pressure (i.e., at SRV safety set-point pressure). More core damage occurring at pressure led to more oxidation and hotter debris temperatures. The hotter temperature of debris exiting the vessel kept the pool on the drywell floor from quenching the debris enough that it could not migrate to the drywell liner. The debris cooled substantially but still managed to move to and melt through the liner.

The cesium release fractions for the cases shown in Figure 9 are compared in Figure 12 below. Cases 2 and 3 both of which lack any mitigation measure involving water (i.e., core sprays or drywell sprays) show the highest release fractions, as expected from a liner melt-through type failure. The fission product releases in these two cases bypass the wetwell after the core exits

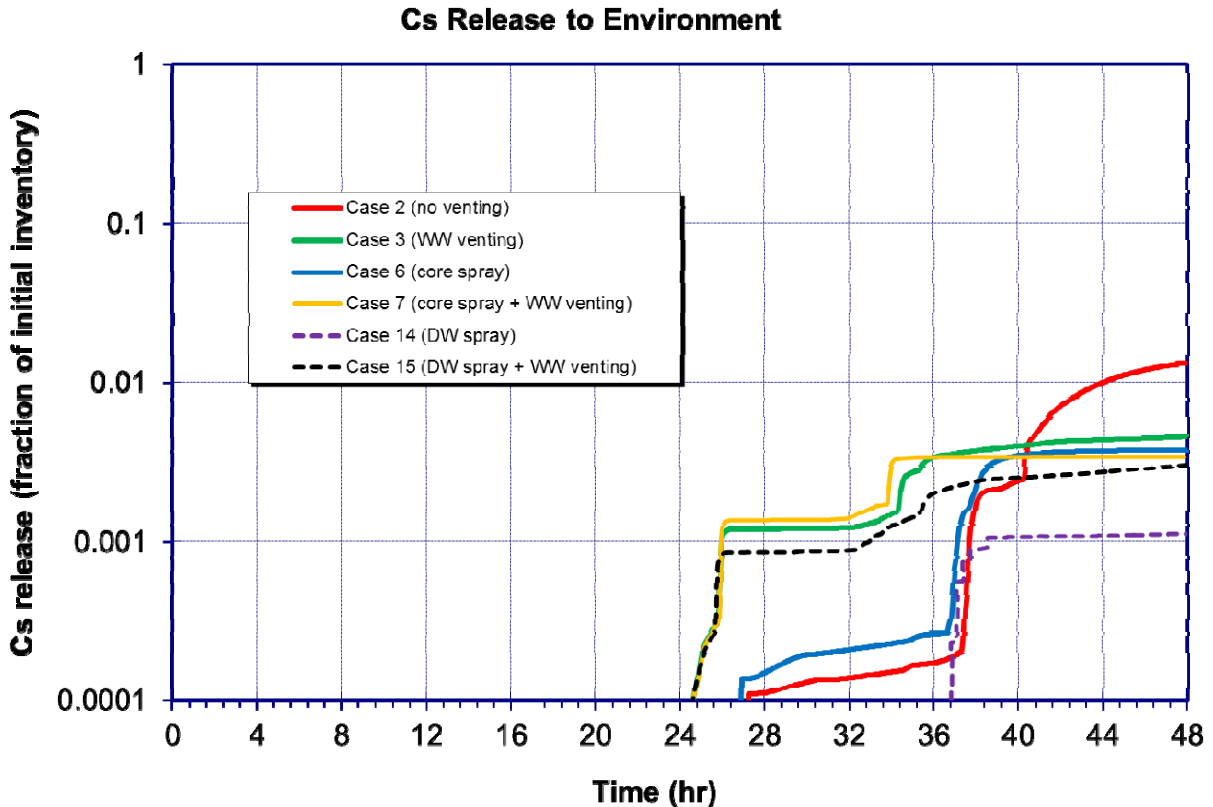


**Figure 12. Comparison of cesium release fractions for selected cases**

the reactor vessel and, as a result, are not scrubbed by the suppression pool. Cases 6 and 7 involving core spray action show moderate effect on fission product attenuation and resulting lower amount of cesium release fractions. The drywell spray action (Cases 14 and 15) show the largest reduction in cesium release fractions. In Case 14, drywell sprays provide significant scrubbing whereas in Case 7, core sprays provides limited scrubbing.

In contrasting Case 15 with Case 14, the difference in the release of cesium to the environment appears to be counterintuitive. Release in Case 15 is higher than in Case 14, even though Case 15 has the supposed benefit of wetwell venting complete with pool scrubbing. There are a couple of reasons for this difference. First, drywell sprays are efficient in Case 14 at keeping containment pressure low enough that there is very little gas leakage past the drywell head flange relative to the amount of gas relieved through the wetwell vent in Case 15. Second, the lower containment pressure in Case 15 (resulting from the wetwell venting) fosters substantially more revaporization of cesium (and other fission products such as iodine) off reactor vessel internals. The vapors escape the reactor and condense to aerosols that are carried towards the wetwell vent. Some of the aerosols are scrubbed in the wetwell pool but not all of them. The aerosols not scrubbed in the pool release to the environment through the wetwell vent. In considering the scrubbing taking place in the wetwell pool during wetwell venting in Case 15, note the flow to the wetwell is through the downcomer vents rather than through a T-quencher. The DF of 10 associated with a downcomer vent is markedly less than the DF of 1,000 associated with a T-quencher. Evidently the increased revaporization of cesium off reactor internals combined with the larger vent flows and less effective wetwell scrubbing in Case 15 lead to the larger releases of fission products to the environment in Case 15 relative to Case 14.

In considering the releases in Case 14, it is worth noting that the drywell head flange leakage model implemented in MELCOR assumes elastic deformation of head bolts and flange seal and does not address inelastic deformation or temperature dependent effects. In reality, the head flange is likely to experience permanent deformation, in part due to aging and other degradation processes over time, and thus the flange gap is likely to widen over time, leading to higher leakage of fission products as well as noncondensable gases.

Cesium release fractions in Figure 12 may be contrasted with those in Figure 13 below, particularly, release fractions pertaining to drywell venting cases (Case 12 and Case 13). Evidently, both Cases 12 and 13 show nearly two orders of magnitude higher release relative to the wetwell venting cases in Figure 12. This is not unusual considering that the drywell venting cases do not have the benefit of pool scrubbing or other forms of decontamination. For the wetwell venting cases considered in the present study, the decontamination factors range between 100 and 300 as shown in Figure 9 above.

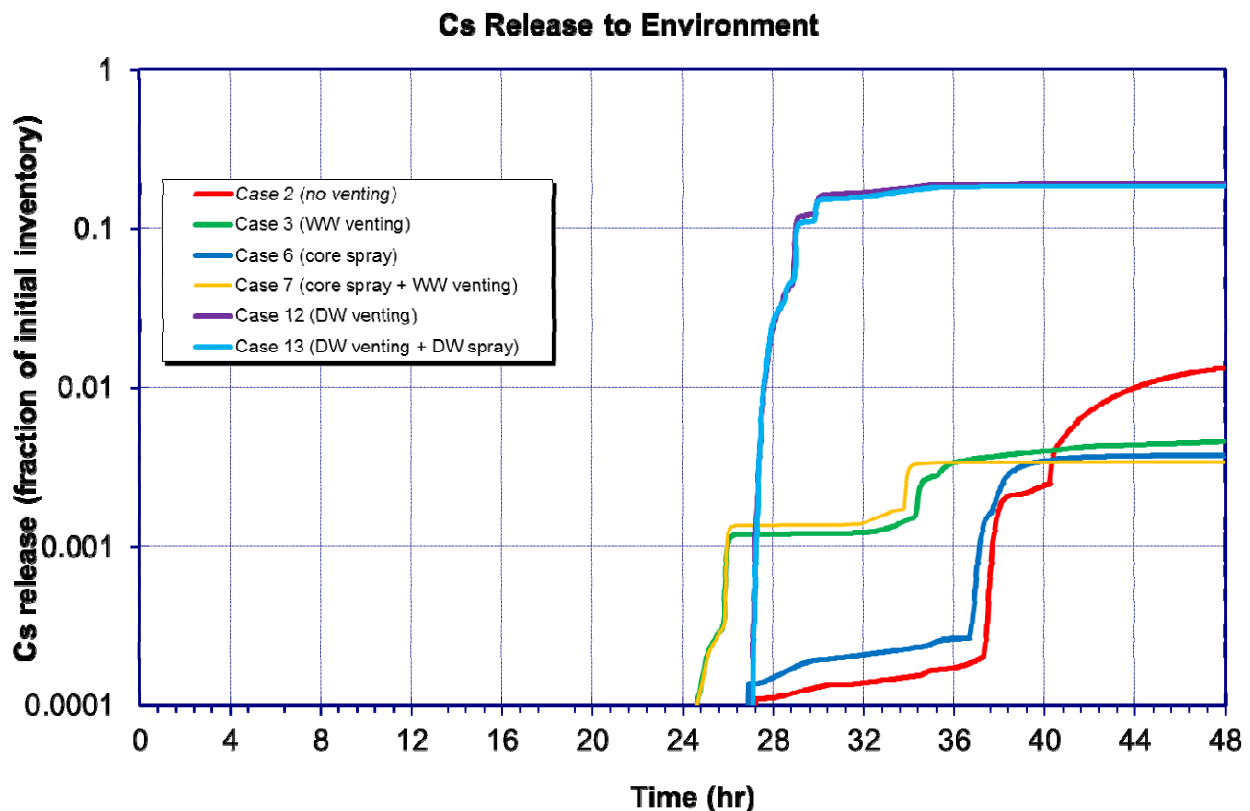


**Figure 13. Comparison of cesium release fractions highlighting drywell venting**

It is important to understand that two fundamental differences were introduced to the accident progression in Cases 12 and 13—both conducive to larger releases to the environment. First, when the MSL rupture took place, fission products escaped the RPV to the drywell rather than to the wetwell for a period of time preceding RPV lower head failure. The fission products introduced to the drywell were available for release through the drywell vent. Second, more core damage occurred at pressure (i.e., at SRV safety set-point pressure). Most all of the cesium released to the environment in the LTSBO calculations can be traced to the revaporization of material deposited on reactor internals during core degradation. The degree

of revaporization increases with increasing time spent at pressure. Consequently, more cesium revaporized from reactor internals when the SRV failure mechanisms were disabled in Case 12. Some of the cesium vapors escaped the reactor vessel and condensed to aerosol, which was available for release through the drywell vent. Cesium and iodine releases to the environment were lower in Case 13 than in Case 12.

Another point is worth noting with regard to drywell/wetwell venting operation. The venting cases presented here do not consider any scenario where the venting is initiated at the wetwell and is transitioned later to drywell. Some plants have reportedly the capability to vent through both wetwell and drywell, and the severe accident management guidance may specify a combination of venting operation. In such a case, the initial release through the wetwell vent will be scrubbed by the suppression pool in the usual course, and the later release through the drywell vent will not be scrubbed. The total release in this case will be lower than that corresponding to a drywell venting only case, and somewhat higher corresponding to a wetwell venting only case. In that sense, release estimates in Figure 13 may be considered bounding.

Note that the fission products are released through several pathways, some of which provide decontamination by natural means (deposition, settling, etc.) or by other means (e.g., suppression pool scrubbing). Other pathways do not provide any decontamination. Depending on the failure mode and location, the various decontamination processes can provide significant attenuation. As two examples, cesium release fractions by different release pathways are shown for two cases in Figure 14 (Case 7) and Figure 15 (Case 14), respectively. In Case 7, nearly 80 percent of cesium release fractions are associated with the wetwell vent path, whereas in Case 14, only about 50 percent is associated with the same path. In creating the input for MACCS calculations, release fractions from different paths are summed up taking into account the appropriate decontamination factors. MACCS calculations are then performed in two sets—one using an external filter with a defined decontamination factor and the other with no filter. The results are contrasted to determine the effect of external filter on consequences.

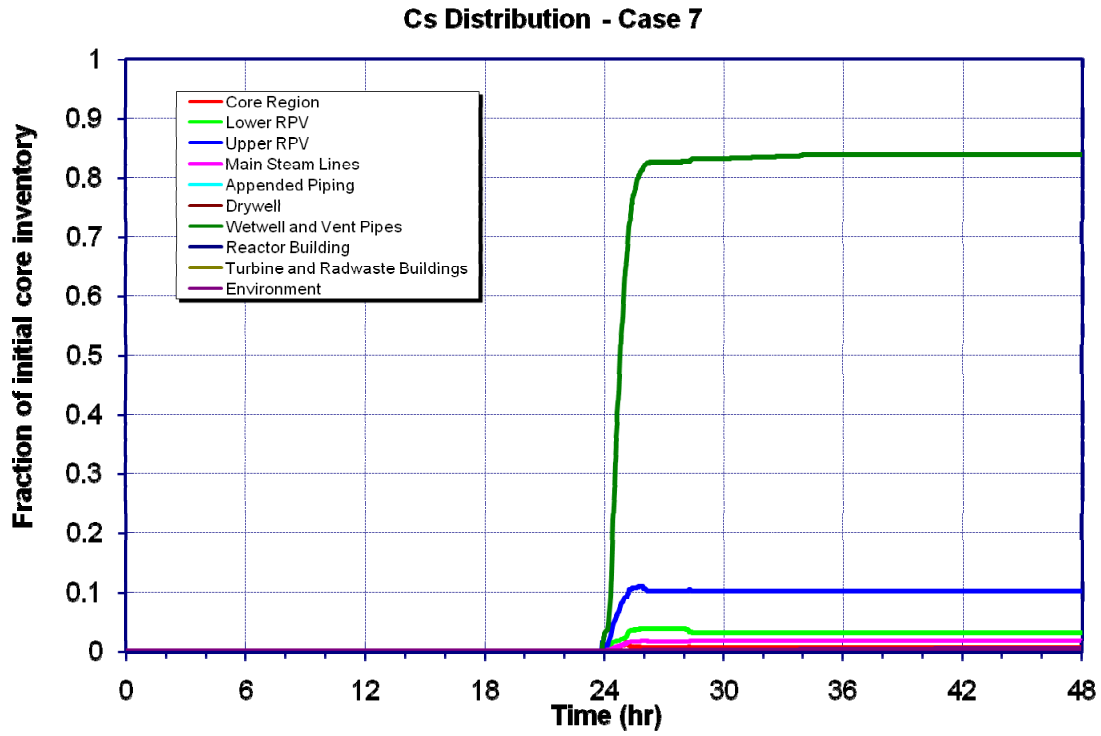


Figure 14. Cesium distribution by various pathways for Case 7

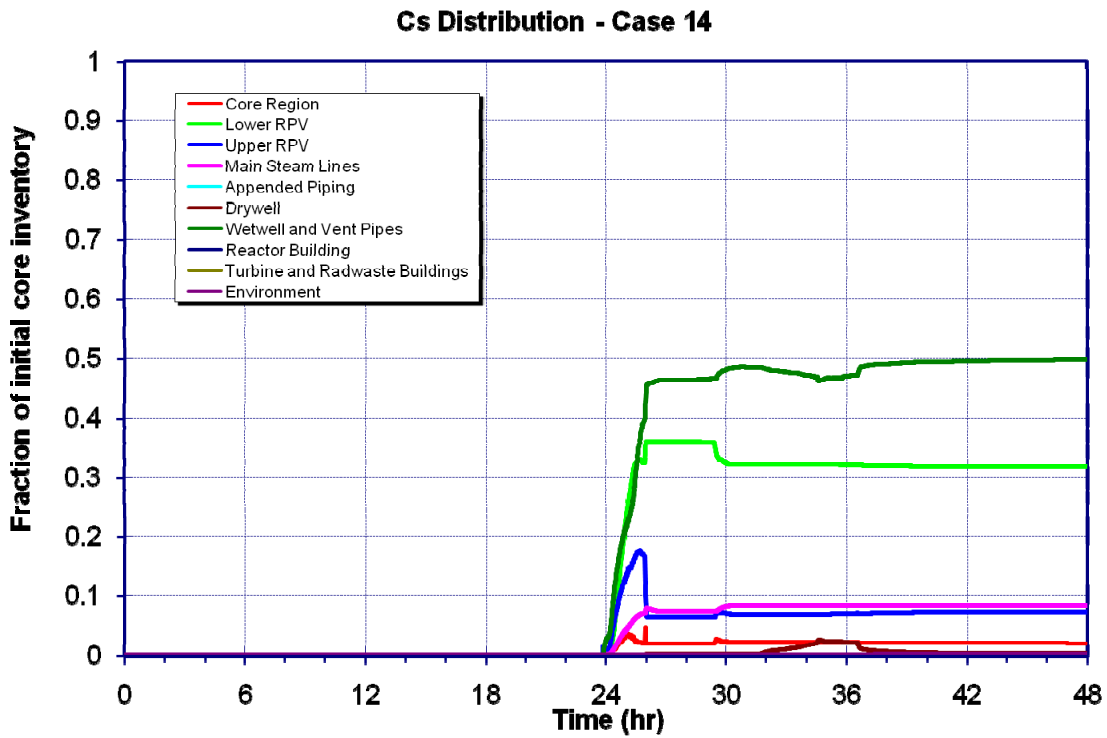
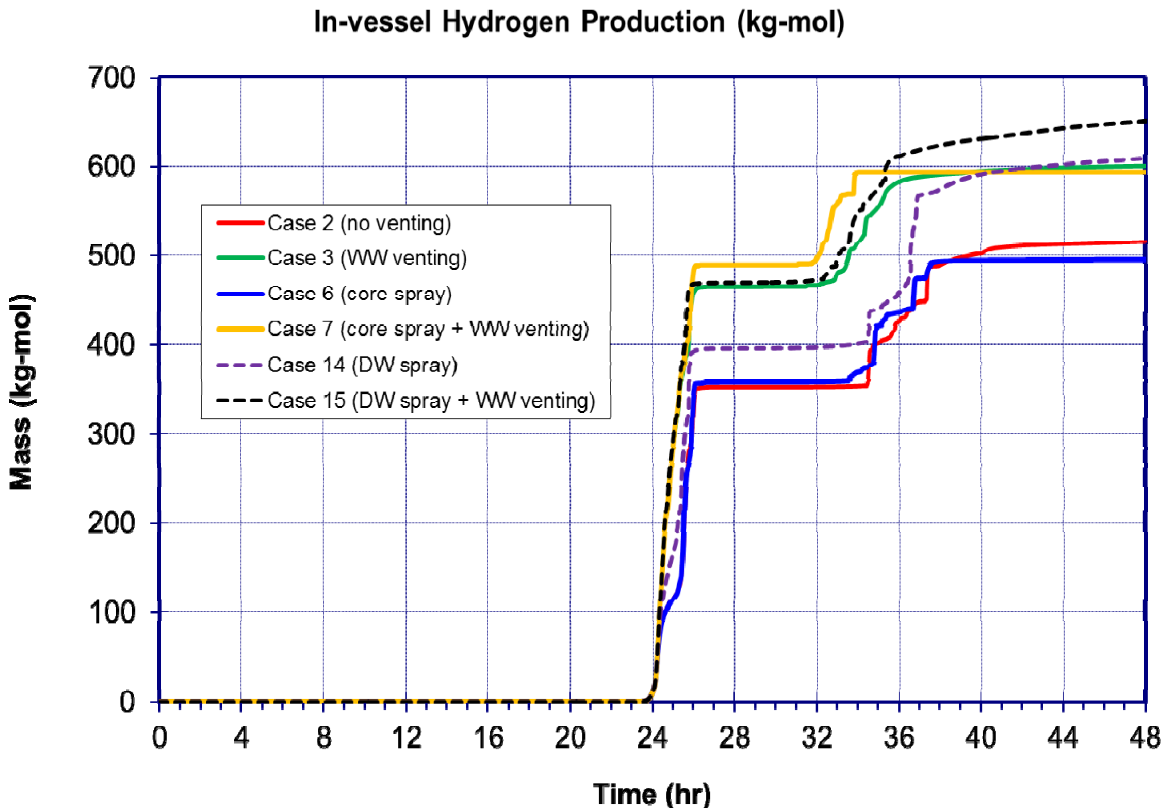


Figure 15. Cesium distribution by various pathways for Case 14

While the presence of water in one form or another has a beneficial effect on fission product scrubbing, this action can also influence the generation of hydrogen as may be evident from the comparison shown in Figure 16 for in-vessel hydrogen production. Consistent with the explanation provided earlier while contrasting venting versus nonventing cases, it is noted that the venting cases considered in the study generally produced 100 to 150 kg-mole (alternatively, 200 to 300 kg) of additional hydrogen in-vessel.



**Figure 16. Comparison of in-vessel hydrogen production for selected cases**

In-vessel generation in Figure 16 shows temporary cessation of hydrogen production as indicated by plateaus (horizontal segments). This is an artifact of MELCOR modeling of clad oxidation. The code considers clad oxidation to be in effect when certain criteria (e.g., minimum pre-oxide layer thickness and minimum temperature) are met. There is also the effect of steam starvation during which clad oxidation cannot take place.

Additional amount of hydrogen and other noncondensable gases (mostly carbon monoxide) are generated from core-concrete interactions (CCI) once the core debris relocates on the drywell floor as can be seen in Figures 17 (for hydrogen) and 18 (for carbon monoxide). The presence of water on the drywell floor has a slowing down effect on CCI and consequent noncondensable gas generation. As a result, less hydrogen and carbon monoxide is produced in all but two cases (Case 2 and Case 3). In these two cases, the amount of hydrogen generated is quite comparable to in-vessel generation amount.

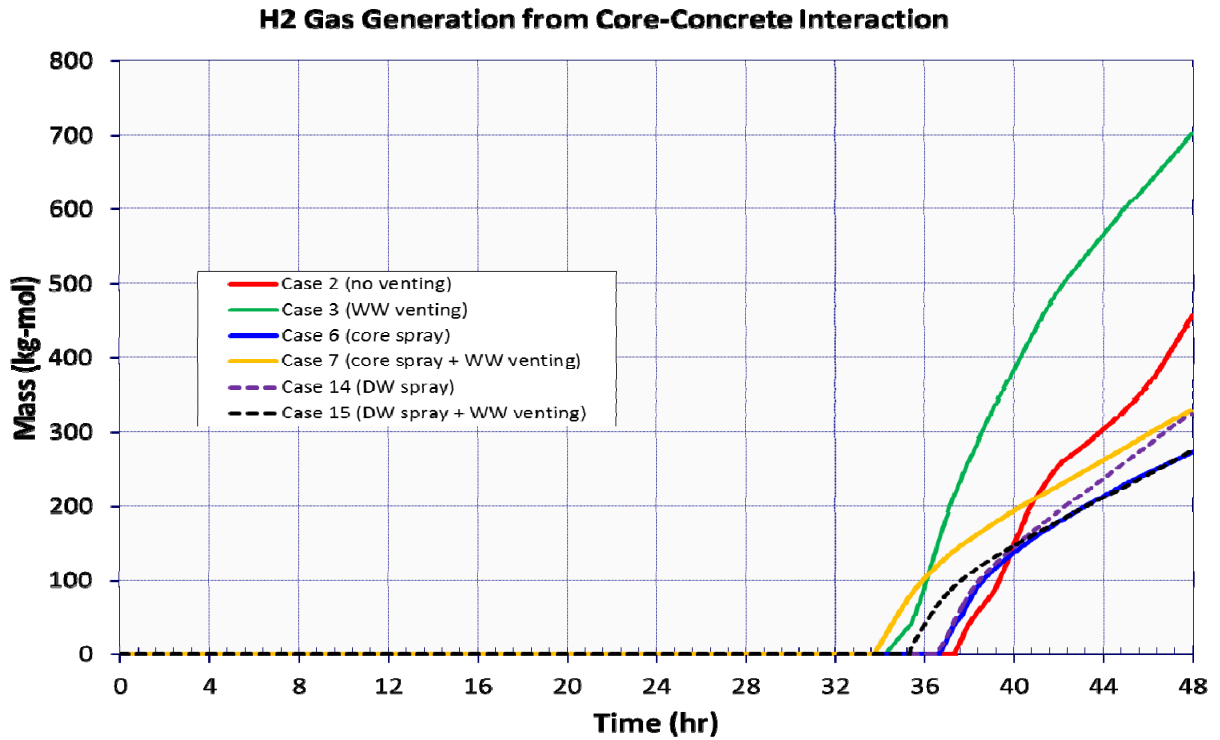


Figure 17. Comparison of ex-vessel hydrogen production

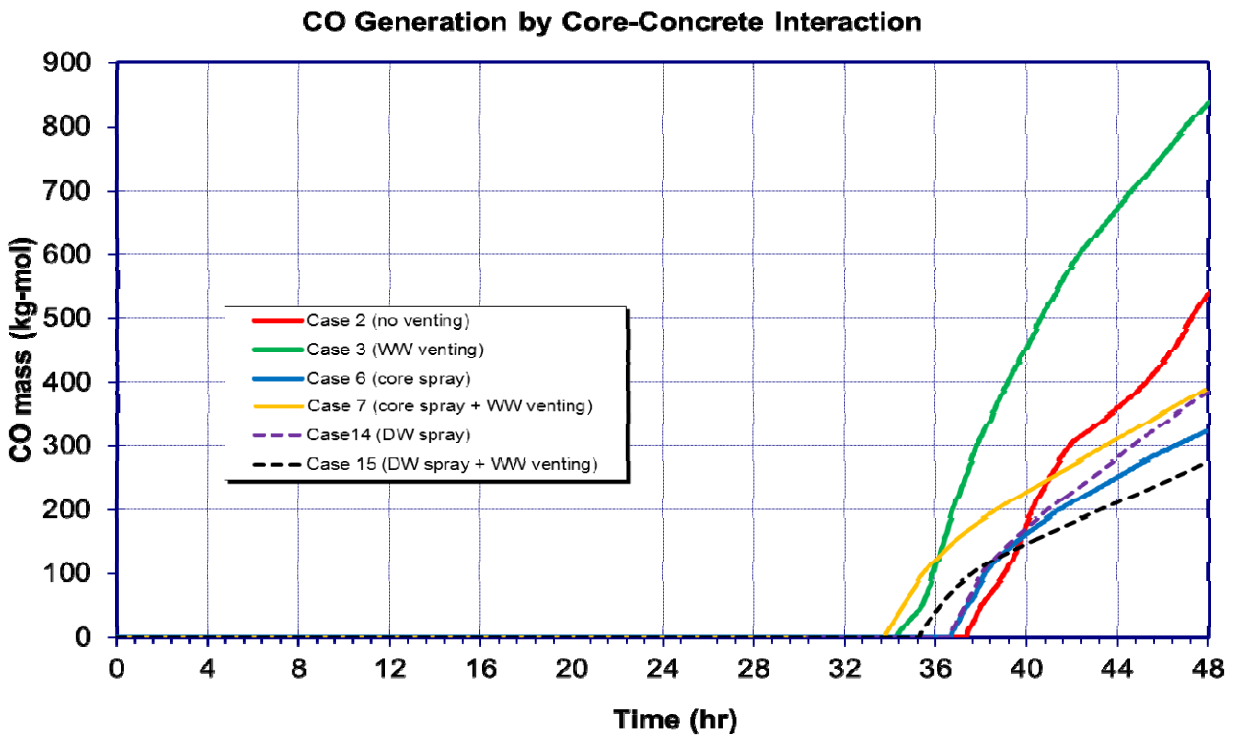


Figure 18. Comparison of ex-vessel carbon monoxide production

## **5.9 Additional MELCOR Cases for Sensitivity Analysis**

Case 1 is identical to Case 2 with the exception of RCIC operation for a 4-hour battery time instead of 16-hour battery time. Likewise, Case 8 is identical to Case 2, except for a RCIC operation with 8-hour battery time. These three cases together are considered as sensitivity cases with variation in RCIC operation time, and are discussed later in more detail.

Case 4 is a venting case where the vent is allowed to cycle between 60 psig (opening) and 45 psig (closing). This case may be contrasted with Case 3 where venting, once opened, remained so through the duration of calculation. Comparison of MELCOR results of these two cases provides an insight of the relative merit of vent cycling.

Case 5 is identical to Case 2 with the added feature that only half of the inventory of the CST is provided for RCIC operation. Case 5 was a sensitivity calculation designed to investigate the dependence of containment pressurization on the source of RCIC suction. RCIC suction is initially from the CST. RCIC suction can optionally be from the wetwell, and by design, an automatic switchover of RCIC suction from the CST to the wetwell would occur as the CST neared depletion. In Case 5, the CST was initialized only half-full, forcing a switchover of RCIC suction to the wetwell.

Cases 8 through 11 represent RCIC operation for an 8-hour battery time. Case 8 is a variation of Case 2, which is already described above. Case 9 is a variation of Case 8 with wetwell venting operation and may be contrasted with Case 3, which has 16-hour RCIC. Case 10 is another variation of Case 8 with core sprays and may be contrasted with Case 6. Finally, Case 11 is a variation of Case 8 with venting and drywell sprays and may be contrasted with Case 7. Generally, the pronounced effect of the duration of RCIC operation is the delay of the onset of core melt progression and subsequent RPV failure.

Case 16 is a variation of Case 2 whereby a 2-CV (control volume) representation of the wetwell was adapted as opposed to 16-CV representation in all previous cases. This is to determine if a coarser representation is adequate for the purpose of MELCOR calculations while still capturing the effect of local temperature variation in the wetwell. Figure 19 shows a comparison of wetwell temperature between a 16-CV representation (Case 2) and a 2-CV representation (Case 16). There is clearly some difference in wetwell temperature between the two cases up to the time of core uncover (about 23 hours), beyond which both representations yield similar wetwell temperature.

Case 17 is a scenario where RCIC operation beyond the battery mission time is allowed by disabling the RCIC failure logic. This scenario is similar to Fukushima Dai-ichi Unit 2 where an extended RCIC operation was observed. Cases 18 through 20 represent sensitivity cases where the drywell spray actuation time was varied (8 hours after SBO in Case 18, 16 hours in Case 19, and 24 hours in Case 20) to examine the spray actuation timing effect on fission product attenuation. These cases were not vented, thus leading to containment overpressure failure. A variation of Case 18 was run with venting in effect (Case 21), which prevented overpressure failure. Note there was no liner melt-through in the last four cases.

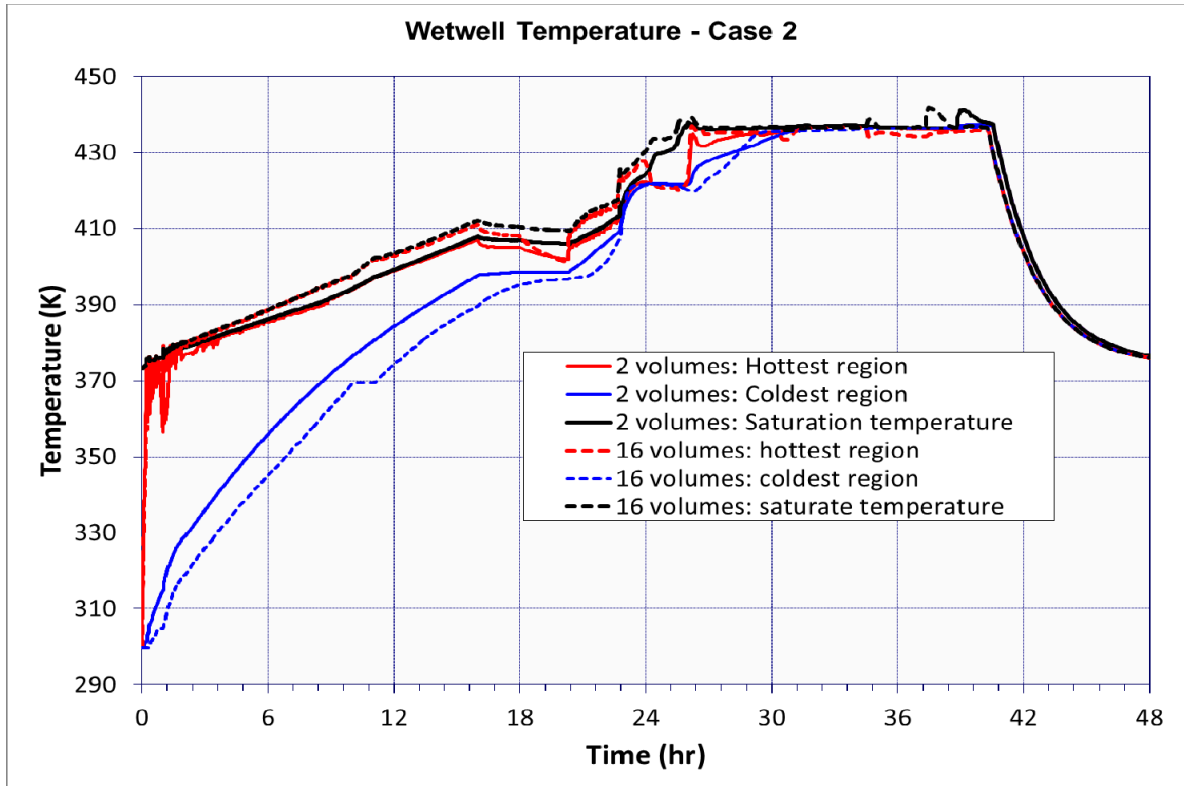


**Figure 19. Comparison of wetwell temperatures between 16-CV and 2-CV representations**

The next three cases involve different failure modes other than the gross lower head failure. Case 22 simulates main steam line creep rupture. Case 23 simulates a traveling in-core probe leak to containment. Case 24 simulates an SRV seal leakage. These various failure mechanisms have been postulated and are being examined to explore the events in Fukushima Dai-ichi plants. Case 25 represents a short-term SBO situation with RCIC failure to start. Note Cases 17 through 25 were all run with RCIC operation of 16 hours, well beyond the battery mission time of 8 hours assumed in these cases. In that sense, these cases may be considered as informed by what was observed in Fukushima Dai-ichi, Unit 2 and Unit 3.

Five additional cases were run to examine additional sensitivities. Case 26 and Case 27 examine the combined effect of vent cycling and drywell spray. Cases 28 through 30 examine the drywell spray flow rate sensitivity.

The MELCOR results pertaining to various sensitivity studies are discussed below.

### 5.10 RCIC Operation Sensitivity

RCIC is designed to provide core cooling, thus delaying core uncover and subsequent accident progression until such time other DC-powered and portable mitigation systems become available. Cooling of the core by RCIC continues, however, for a period defined by the battery mission time. Following failure of RCIC to operate, the core uncover will begin. As mentioned previously, baseline calculations were performed with 16-hour RCIC operation time (multiple cases), one sensitivity calculation (Case 1) was performed with RCIC operation time of 4 hours

(so the results can be compared with the SOARCA results), and a limited number of calculations (Cases 8 through 11) were performed with RCIC operation time of 8 hours. Some of these cases involved consideration of additional mitigation measures such as spray.

Three cases (Case 1, Case 2, and Case 8)—all with no additional prevention or mitigation features—are compared here to provide an understanding of RCIC operation sensitivity. Figure 20 shows, as an example, the comparison of hydrogen production at reactor vessel failure for different duration of RCIC operation. The primary benefit of extended RCIC operation time is to delay the reactor vessel failure, thereby gaining additional time to implement other prevention and mitigation measures, as they become available.

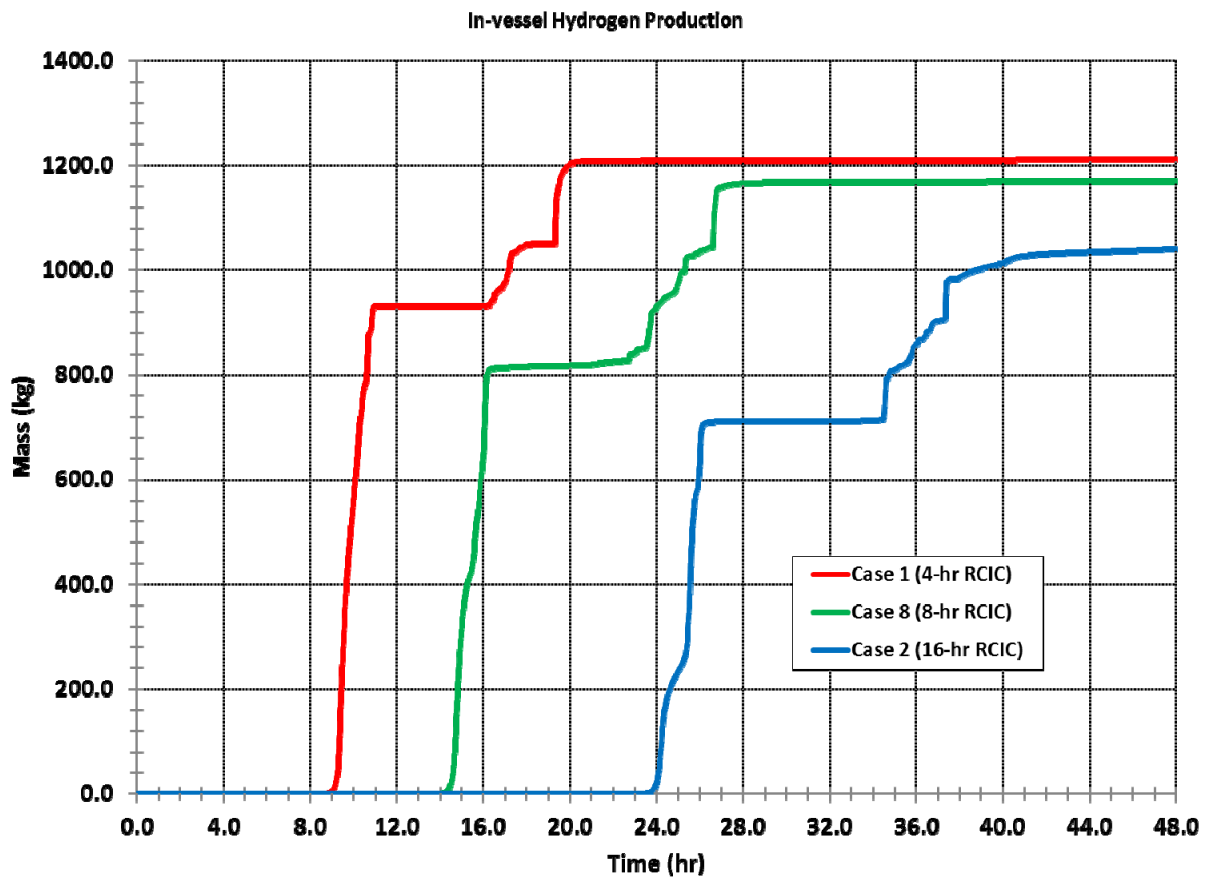


**Figure 20. Comparison of in-vessel hydrogen production for various RCIC durations**

The difference in hydrogen production between these cases is evident. With shorter duration RCIC (e.g., 4 hours), the core is at a higher decay power than that with a longer duration RCIC. This difference in decay power can alter the accident progression. There is a direct correlation between cladding temperature and in-vessel hydrogen production, and it is not uncommon to see a change in cladding temperature on the order of 200 to 300 degrees in these calculations. The corresponding change in hydrogen production could be on the order of 200 kg or so. Note that since none of these cases consider any mitigation measure involving water addition, they all lead to containment failure by liner melt-through—a bypass type of failure mode in which an external filter, whether at the wetwell end or at the drywell end, provides no benefit of fission product decontamination.

## 5.11 Effect of Spray

To illustrate the effect of spray, cesium release fractions for four cases (Case 2, Case 3, Case 6, and Case 14) were contrasted, all with 16-hour RCIC operation. Of these, Case 6 involved core spray actuation with a 300 gpm flow rate at vessel failure. Case 14 involved drywell spray actuation, also with a 300 gpm flow rate, but at 24 hours (shortly after vessel failure). Case 2 involved no venting or spray, and Case 3 involved wetwell venting but no spray. Core spray actuation at vessel failure was selected based on the consideration that the hookup of a transportable fire water system may not be feasible when the reactor vessel is at high pressure. Cesium release fractions for these cases are plotted in Figure 21 below. Needless to say, with spray action, the liner melt-through mode of failure is prevented.

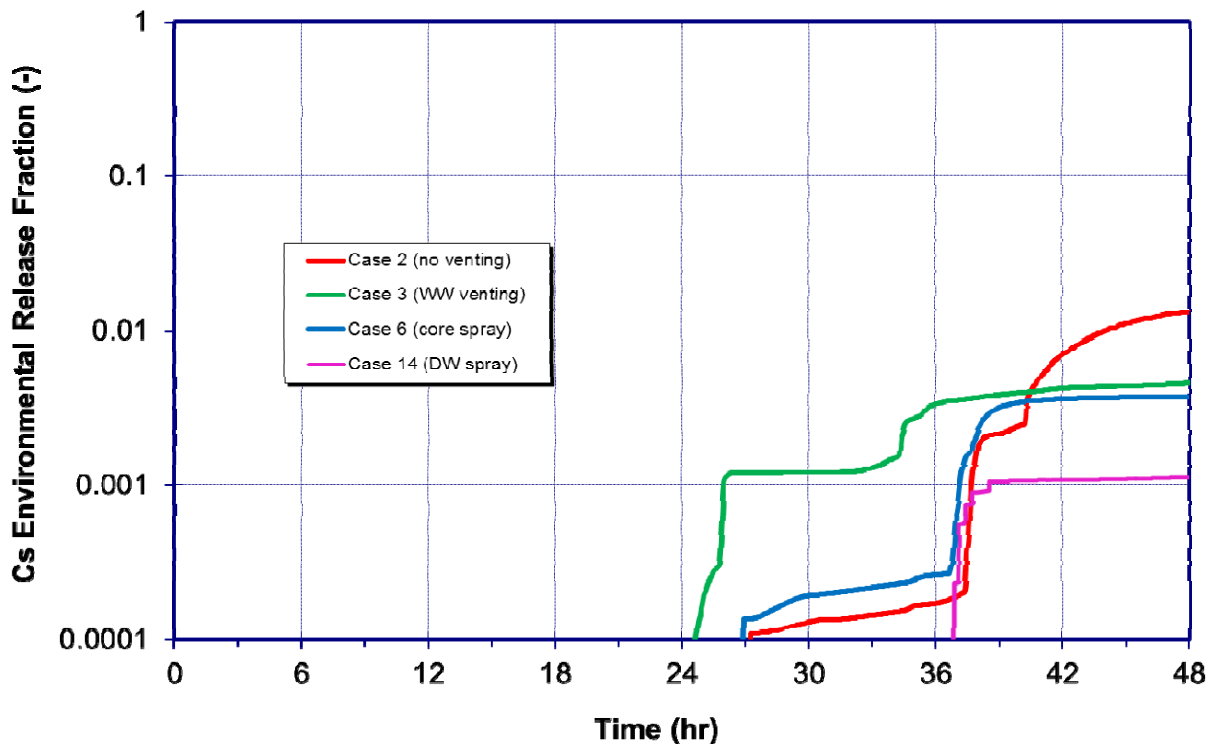


Figure 21. Comparison of cesium release fraction showing spray effect

A comparison of cesium release fractions in Figure 21 shows gradual reduction of releases from no venting case to venting to core spray and finally, to drywell spray. Venting alone or core spray alone provides about a two-thirds reduction in releases relative to the no venting case, whereas the drywell spray action provides a considerably higher reduction.

## 5.12 Combined Effect of Venting and Spray

Several cases were run where the venting was in effect. These cases include venting in either a passive mode (i.e., vent once opened remains open) or an active mode (i.e., vent opening and closing are cycled through operator action), in combination with spray action (core or drywell). Venting in passive mode is initiated at a drywell pressure exceeding 60 psig or about 75 psia (design pressure). Vent opening in active mode is initiated likewise at a pressure of 60 psig and closing is initiated when the drywell pressure drops to 45 psig.

Figure 22 provides a comparison of cesium release estimates for combined cases of venting and spray (Case 7 with venting and core spray and Case 15 with venting and drywell spray) contrasted to Case 2 (no venting or spray). Unless otherwise stated, the venting is always considered through wetwell. As long as the drywell is at a higher pressure, that will be the preferential vent path. If the suppression pool level is increased significantly, the wetwell vent path cannot be used, in which case fission products will be transported through drywell vent. Note in such a case (Case 12), fission products will not be scrubbed as the releases bypass the suppression pool and, as such, the releases will be much higher than those of the wetwell vent cases.

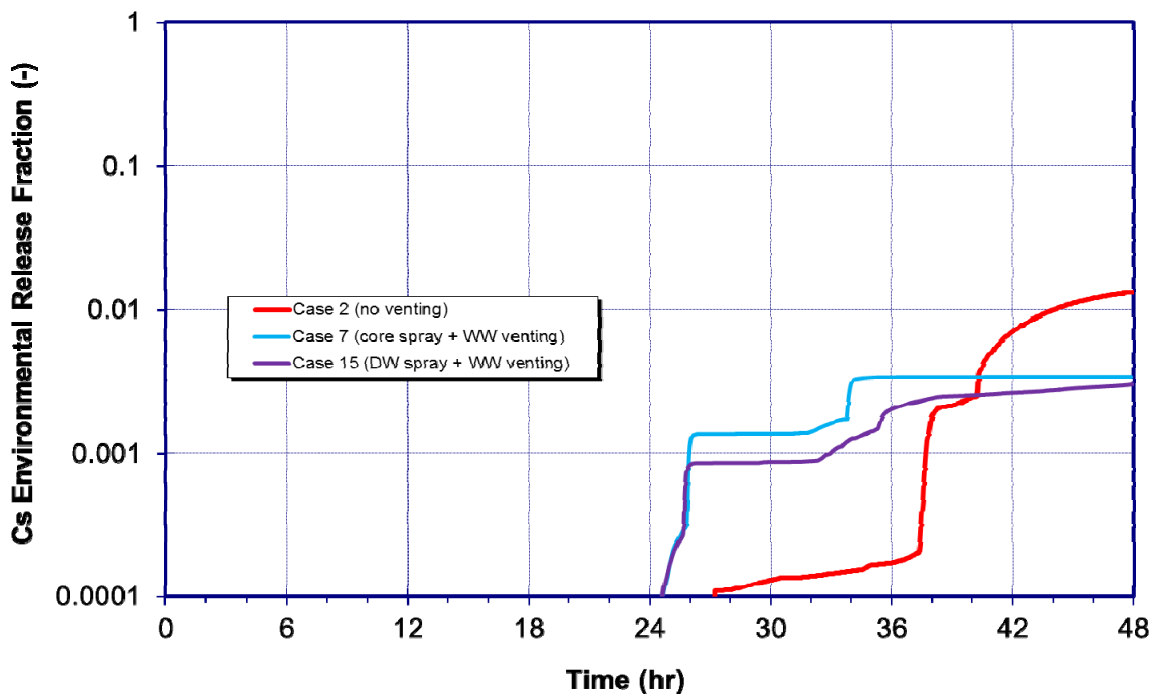


**Figure 22. Cesium release fraction showing combined venting and spray effects**

When compared with Figure 21 above, there appears to be modest additional reduction of releases in the cases with combined venting and spray actions. Core spray, upon actuation at or shortly after vessel failure, provides some degree of cooling of the remainder of the degraded core that may still be held up structurally inside the vessel. Moreover, the water from core spray finds its way to the drywell floor, thus effectively flooding the cavity. Because the core spray flow rate is not high, the pool created in the drywell is not expected to be deep. Also, the water will likely be saturated by the time it ends up on the drywell floor. Nevertheless, fission products will be modestly scrubbed by the flooded cavity before they are transported to the wetwell and go through suppression pool scrubbing. This appears to be the reason for getting a nominally incremental attenuation by a combination of venting and core spray actions.

The drywell spray action, likewise, provides scrubbing of the airborne fission product aerosols. When combined with venting, any additional attenuation of fission products depends on the resulting aerosol size distribution and the corresponding suppression pool scrubbing efficiency as the fission products are transported through the wetwell vent. In the particular example shown in Figure 22 (reference Case 15), there was no incremental benefit with the combined

venting and spray action. Note the drywell spray was initiated after venting in Case 15 so the initial aerosol inventory did not benefit from the spray action. Generally, a significant amount of the initial fission product inventory will likely go through the wetwell prior to drywell spray actuation. This may be the reason for a slightly lower decontamination in Case 15 when compared to Case 14. In cases where venting is initiated after spray actuation, there appears to be a nominally incremental attenuation by a combination of venting and drywell spray action in contrast to spray action alone, much like the combined effect of core spray and venting.

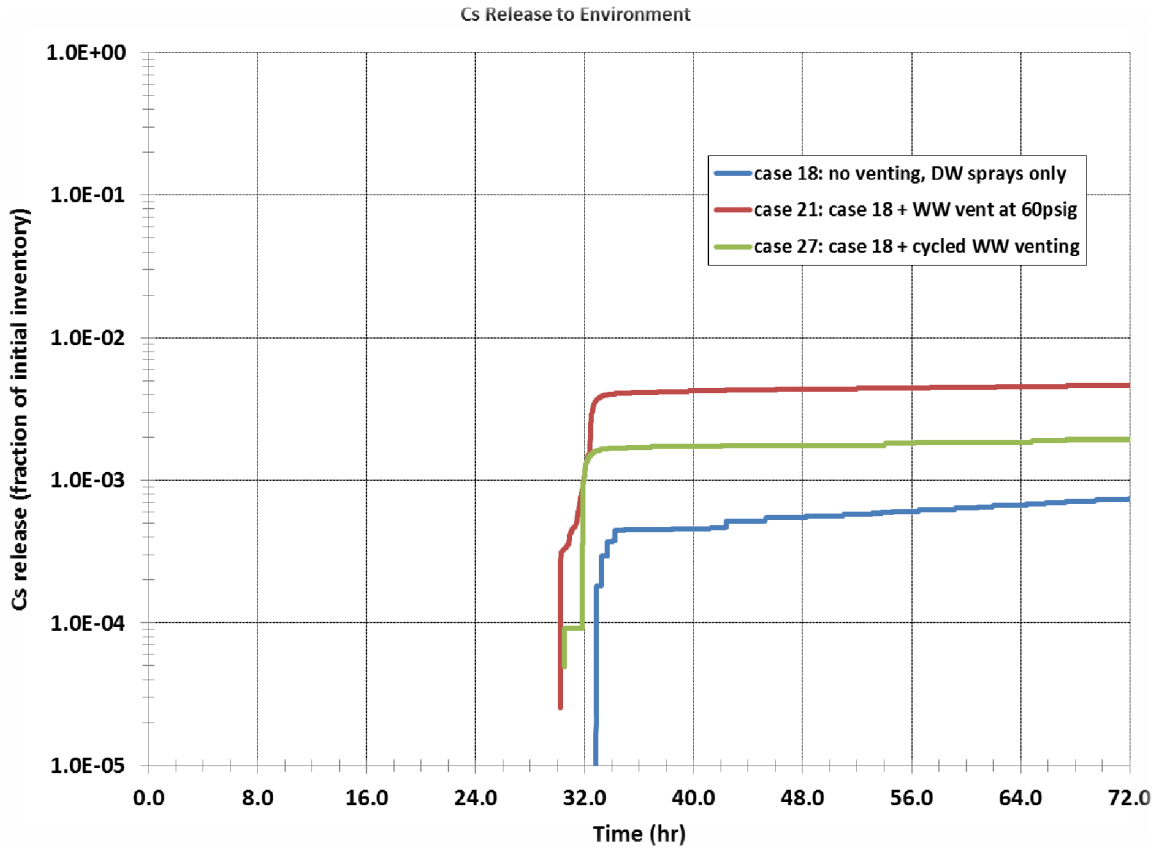
Another grouping of selected MELCOR case runs was examined to determine the relative effect of vent cycling versus venting once and keeping it open.

Figure 23 shows the comparison between once-opened vent and vent cycling cases with and without spray action. Case 18 in this figure is no venting, Case 21 is that of once-opened wetwell vent, and Case 27 that of vent cycling—all with spray action. The MELCOR results indicate slightly smaller releases in the case of vent cycling when compared to once-opened vent cases; however, both are within the same order of magnitude. Note that EPRI's preliminary findings indicate vent cycling to be more effective in reducing fission product release relative to once-open venting. It appears that EPRI's analysis may have accounted for only the wetwell releases whereas in their model, both drywell and wetwell release paths were considered.

Note this report makes no a priori assumption regarding the implementation of vent cycling operation (i.e., feasibility of such operation, effectiveness and timeliness of operator actions in an accident situation). Even if vent cycling is demonstrated to be effective, the feasibility of its operation needs to be carefully examined.

### **5.13 Drywell Spray Sensitivity**

The drywell spray sensitivity was explored in two different ways. First, the effect of drywell spray actuation timing was investigated in a series of three runs, all without venting. Case 18 represents drywell spray actuation time of 8 hours, Case 19 represents an actuation time of 16 hours, and Case 20 an actuation time of 24 hours. Second, the spray flow rate sensitivity was explored by varying the flow rate from 100 gpm to 1,000 gpm. For this, the 24-hour core spray actuation with 300 gpm flow rate (Case 14) was selected as the base case. Case 28 was a variation of Case 18 with 100 gpm flow rate; Case 29 a variation with 500 gpm flow rate; and finally, Case 30 a variation with 1,000 gpm flow rate.



**Figure 23. Comparison of cesium release fractions for vent once and vent cycling cases**

For the spray actuation time sensitivity, cesium release fractions are plotted in Figure 24 below. Generally, late spray actuation provides less opportunity for scrubbing as may be evident by comparing Case 19 and Case 20 results individually with Case 18 results. The release estimates, however, are within the bounds of uncertainties so it cannot be readily concluded that when the drywell spray is used as the only mitigation measure, its actuation time impact significantly the release estimates. Note the early actuation of drywell spray may have a concomitant effect of flooding the cavity and the pedestal region to the point that the wetwell venting becomes ineffective.

As mentioned earlier, the three cases considered for the spray actuation timing sensitivity do not consider venting, meaning these cases eventually lead to overpressure failure of the containment through head flange leakage. The head flange leakage model in MELCOR considers only elastic deformation of bolts, based on pressure differential. As a result, the flange opens and closes during the transient as an artifact of the model, thus limiting somewhat the releases. The timing of opening and closing of the flange is not the same in every case of drywell spray actuation, and that explains the different trend in releases between Case 19 and Case 20.

For the flow rate sensitivity analysis, cesium release fractions are plotted in Figure 25 below. Within the flow rates considered in the present analysis, there does not appear to be a large sensitivity with regard to release estimates. The 100 gpm flow rate (Case 28)—more like sprinkling flow—provides the least amount of fission products scrubbing and hence the most

release, albeit still less than 1 percent at 48 hours. The higher flow rates (Case 14 with 300 gpm as the best case, Case 29 with 500 gpm, and Case 30 with 1,000 gpm) result in

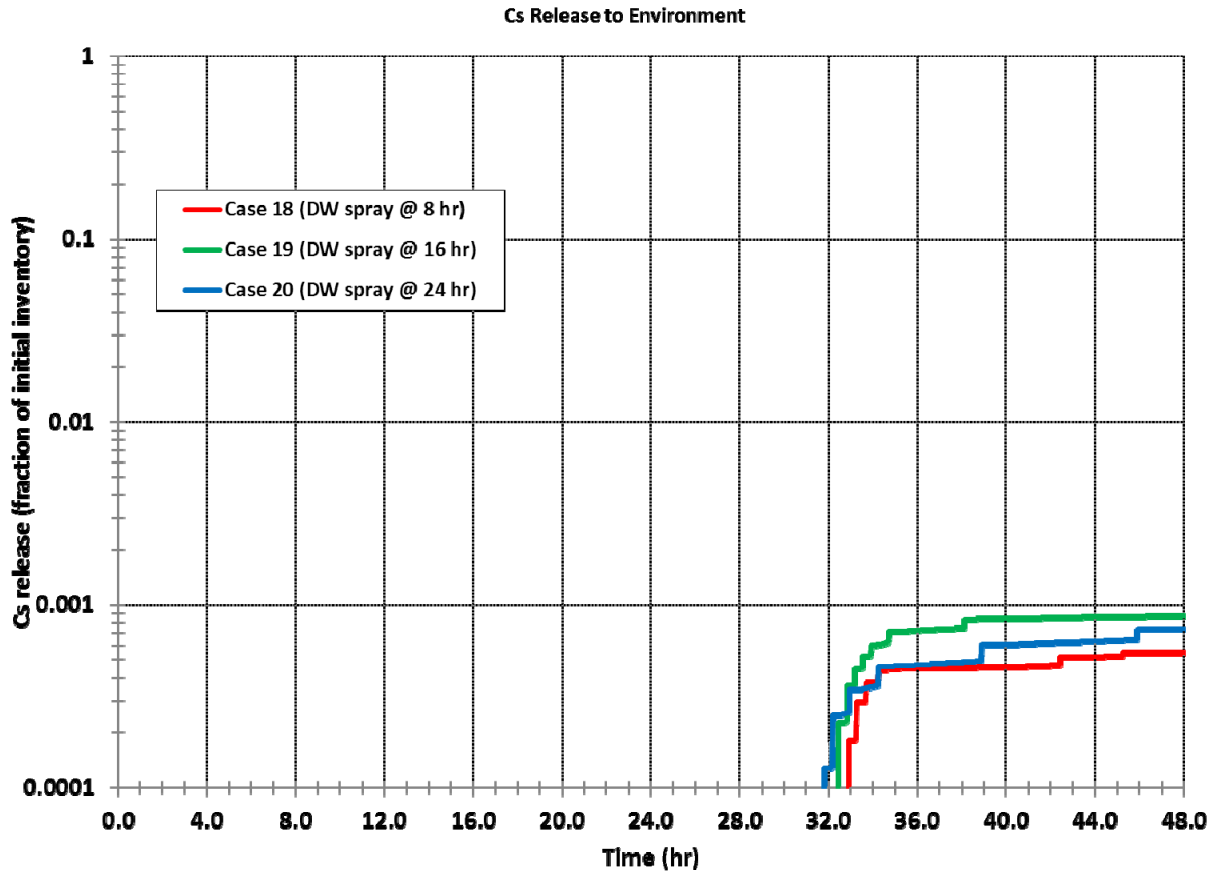


**Figure 24. Effect of drywell spray actuation time on cesium release fraction**

lesser release amounts (between 0.05 to 0.1 percent of initial inventory). Given the trend, a much higher flow rate is expected to provide further reduction in release amounts.

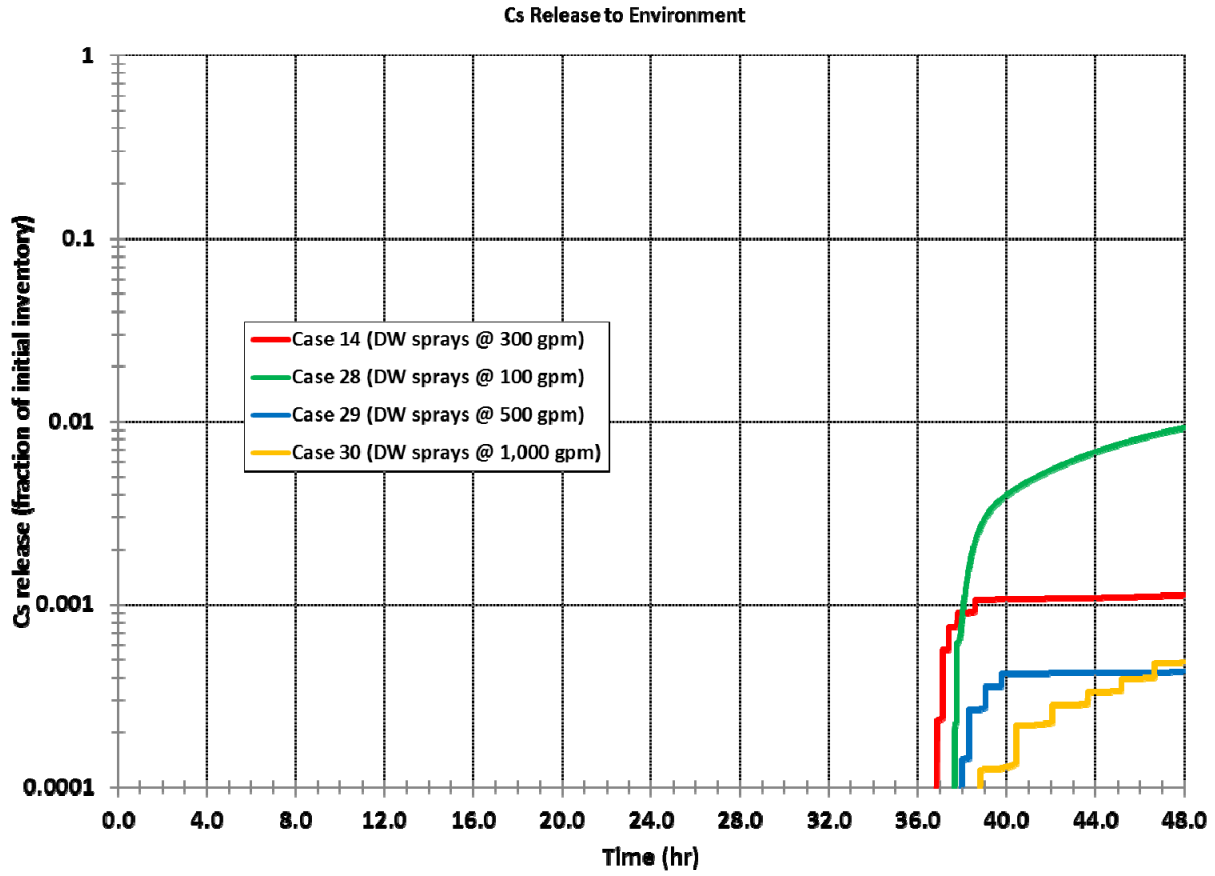


**Figure 25. Effect of drywell spray flow rate on cesium release fraction**

## 6. CONCLUSIONS FROM MELCOR ANALYSIS

The MELCOR analysis presented above, when considered in combination with the MACCS analysis in Enclosure 5b, makes a compelling technical argument for a strategy to mitigate radiological consequences of severe accidents in BWR Mark I containments that includes a combination of venting and spray action, supplemented further by the installation of an external filter. In other words, the MELCOR/MACCS analyses provide a technical basis to support Option 3 in the regulatory analysis. The external filter aspect of the technical basis is discussed further in the context of the MACCS analysis (Enclosure 5b) of health effects and property damage consequence (land contamination). The MELCOR analysis presented here leads to the following specific conclusions on containment venting and other mitigation actions.

- A combination of venting and spraying (or any mitigation action including water on the drywell floor) is required for an effective strategy for mitigating radiological releases. Venting alone or spraying alone does not provide sufficient reduction in radiological releases. The combined action results in significant reduction of fission product release. In some accident sequences, venting and provision of water, when supplemented with natural decontamination processes (e.g., fission product deposition on structural surfaces), can provide an overall decontamination factor approaching 1,000.
- An external filter is capable of providing additional fission product attenuation of already scrubbed aerosols (by spray or flooding action, or by suppression pool scrubbing). Thus, external filtering has a direct influence on reducing further the amount of fission product release to the environment, and consequent reduction in health effects and land contamination.
- Venting through the wetwell is preferred as it provides an opportunity for fission product scrubbing in the suppression pool. Pool scrubbing efficiency can be appreciable (decontamination factor in the range between 100 and 300 in the MELCOR analysis). Venting through drywell does not have pool scrubbing benefit. As such, if the drywell vent is used for the purpose, external filtration would be necessary to reduce the amount of fission product release to the environment.
- Venting prevents overpressurization failure, and excessive buildup of hydrogen and other noncondensable gases in the reactor building and other areas, thereby providing an effective means of combustible gas control. Though the hydrogen issue is not the focus of the current study, this particular insight lends further credibility to the efficacy of venting.
- MELCOR analysis, results therein, and the conclusions drawn above are consistent with the insights provided in the EPRI report [14] with one notable exception. MELCOR calculations do not show vent cycling to be any more effective than once-open venting. The release estimates in both cases are on the same order of magnitude. Preliminary EPRI calculations concluded vent cycling to be more effective. Even if vent cycling is demonstrated to be effective, the feasibility of its operation needs to be carefully examined. Note that the insights in the EPRI report recognize that an external filter can further reduce the fission product release to the environment—consistent with the conclusion from MELCOR/MACCS analysis.

- Limited sensitivity analysis carried out indicates that the release estimates are not sensitive to spray flow rate in the low flow regimes that are practically achievable in an accident situation. The estimates are also not particularly sensitive to spray actuation timing. Early actuation of drywell sprays may have a concomitant effect of flooding the cavity and the pedestal region to the point that the wetwell venting becomes no longer effective.

## 7. REFERENCES

- [1] U.S. Nuclear Regulatory Commission, "Recommendations for Enhancing Reactor Safety in the 21st Century, The Near-Term Task Force Review of Insights from the Fukushima Dai-ichi Accident," July 12, 2011.
- [2] MELCOR Computer Code Manuals, Version 1.8.6, Vol. 1: Primer and Users' Guide, NUREG/CR-6119, Vol. 1, Rev. 3, SAND 2005-5713, September 2005.
- [3] D. Chanin, M. L. Young, J. Randall, "Code Manual for MACCS2: User's Guide," NUREG/CR-6613, Vol. I (1998).
- [4] State-of-the-Art Reactor Consequence Analyses (SOARCA) report, NUREG-1935, January 2012.
- [5] Fukushima Daiichi Accident Study (Status as of April 2012), SAND2012-6173, July 2012.
- [6] Ramamurthi, M., and M. R. Kuhlman, "Final Report on Refinement of CORSOR—An Empirical In-Vessel Fission Product Release Model," Battelle Report, October 31, 1990.
- [7] B. Clement, T. Haste "Comparison Report on International Standard Problem ISP-46 (FPT1)" Note Technique SEMAR 03/021, 2003.
- [8] D.A. Powers, J.E. Brockmann, A.W. Shiver, VANESA: A Mechanistic Model of Radionuclide Release and Aerosol Generation during Core Debris Interactions with Concrete, NUREG/CR-4308, Sandia National Laboratories, Albuquerque, NM, July 1986.
- [9] F. Gelbard, "MAEROS User Manual," NUREG/CR-1391, Sandia National Laboratories, Albuquerque, NM, December 1982.
- [10] SPARC-90: A Code for Calculating Fission Product Capture in Suppression Pools, NUREG/CR-5765, October 1991.
- [11] Cunane, J. C., et al., "The Scrubbing of Fission Product Aerosols in LWR Water Pools Under Severe Accident Conditions - Experimental Results," EPRI NP-4113-85, Electric Power Research Institute, Palo Alto, California, 1985.
- [12] Owczarski, P. C., and W. K. Winegardner, "Validation of SPARC, A Suppression Pool Aerosol Capture Model." Paper IAEA-SM-281/29, presented at IAEA International Symposium on Source Term Evaluation for Accident Conditions, Columbus, Ohio, 1985.
- [13] D. A. Powers and J. L. Sprung, "A Simplified Model of Aerosol Scrubbing by a Water Pool Overlying Core Debris Interacting With Concrete," NUREG/CR-5901, SAND92-1422, Sandia National Laboratories, Albuquerque, New Mexico, 1992.
- [14] Electric Power Research Institute, "Investigation of Strategies for Mitigating Radiological Releases in Severe Accidents: BWR Mark I and Mark II Studies," 2012 Technical report, September 2012.